

Characterization of Compression Moulded CF-PEEK Recyclate to Enhance Process Understanding

Stefan Pariyski

Wissenschaftliche Arbeit zur Erlangung des Grades M.Sc.

Themenstellende/r	Univ.-Prof. Dr.-Ing. Klaus Drechsler Lehrstuhl für Carbon Composites
Betreuer	Jan Teltschik, M.Sc. Lehrstuhl für Carbon Composites
Eingereicht von	Stefan Pariyski
Eingereicht am	01.09.2022 in Garching bei München

Technische Universität München
Fakultät für Luftfahrt, Raumfahrt und Geodäsie
Lehrstuhl für Carbon Composites
Boltzmannstraße 15
D-85748 Garching bei München

Tel.: +49 (0) 89 / 289 – 15092

Fax: +49 (0) 89 / 289 – 15097

Email: info@lcc.lrg.tum.de

Web: www.lrg.tum.de/lcc

Aufgabenstellung

Chair of Carbon Composites
Department of Aerospace and Geodesy
Technical University of Munich



Master's Thesis

Characterization of compression moulded CF-PEEK recycleate to enhance process understanding

During the production of CFRP structures using Thermoplastic Automated Fibre Placement (TP-AFP) on an industrial scale, there are waste residues of up to 20%. These high quality tape offcuts are today disposed of as hazardous waste. At the same time, the high prices of carbon fibre reinforced materials are a limiting factor for the economic use of carbon composites. Therefore, there is a need for a process that enables the further processing of the material residues. For this purpose, at the Chair of Carbon Composites, a vacuum-assisted pressing process for long-fibre-reinforced thermoplastics (LFT) from tape offcuts with subsequent integration into the AFPisc process is being developed within the project REUSELAGE.

Within the scope of the Master's thesis, compression moulded LFT specimens made of CF-PEEK recycleate are to be comprehensively mechanically characterised. The material properties are to be analyzed depending on process parameters and part thickness in order to be able to draw conclusions on the optimal process window as well as limits of possible part geometries.

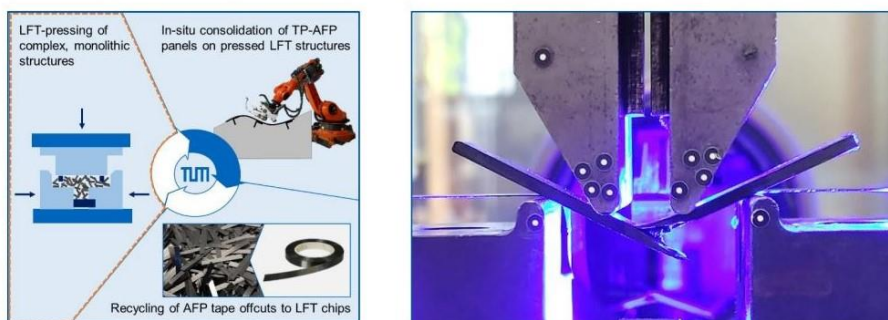


Figure: Process diagram of LFT pressing with AFP as follow-up process; 4-Point Bending of LFT specimens.

Research focus of the thesis

- Research on the state of the art regarding
 - Recycling of carbon fibre reinforced high performance thermoplastics
 - LFT moulding technologies
 - Test specifications for LFT
- Mechanical Characterization of LFT plates
 - Manufacturing of LFT specimens by compression moulding
 - Planning and execution of mechanical tests (Flexural, tensile, compression and ILS testing)
 - Interpretation of test results with regard to process parameters and specimen thickness
- Documentation and presentation

Requirements

- Basic knowledge of fibre composites advantageous
- Structured and independent work ethic
- The work can be carried out in German or English

Starting date: Now

For more details please contact:

Jan Teltschik, Room MW 1407, FSZ, Tel. +49 89 / 289 – 15789, jan.teltschik@tum.de

Ehrenwörtliche Erklärung

Ich erkläre hiermit ehrenwörtlich, dass ich die vorliegende Arbeit selbstständig und ohne Benutzung anderer als der angegebenen Hilfsmittel angefertigt habe; die aus fremden Quellen (einschließlich elektronischer Quellen) direkt oder indirekt übernommenen Gedanken sind ausnahmslos als solche kenntlich gemacht.

Die Arbeit wurde in gleicher oder ähnlicher Form noch keiner anderen Prüfungsbehörde vorgelegt.

München, 01.09.2022

.....

Ort, Datum

Unterschrift

Übersicht

Ziel dieser Masterarbeit ist es, den recycelten Langfaser-Thermoplast (rLFT) aus kohlenstofffaserverstärktem Polyether-Ether-Keton (CF-PEEK) zu charakterisieren, der bei dem Formpressen im Rahmen eines geschlossenen Recyclingprozesses für thermoplastische Verbundwerkstoffe entsteht. Die Abfälle und Verschnitte, die bei einem thermoplastischen automatischen Faserlegeverfahren mit In-situ-Konsolidierung anfallen, werden zusammen mit den Abfällen aus der Herstellung der dafür benötigten unidirektionalen CF-PEEK-Tapes auf die notwendige Faserlänge zugeschnitten und unter Vakuum, Druck und Temperatur in die gewünschte Form gepresst. Durch Biegeversuche wird der Parameterraum des Prozesses analysiert und ein optimaler Satz von Prozessparametern gefunden. Für die Materialcharakterisierung wurden fünfzehn Platten aus CF-PEEK-Chips formgepresst, darunter Platten mit unterschiedlichen Dicken und eine Platte, die ohne Vakuum verarbeitet wurde. Anhand von sieben verschiedenen mechanischen Tests wurden sechs Festigkeiten, drei Elastizitätsmoduln, ein Schubmodul und eine Querkontraktionszahl ermittelt, die für die Modellierung des formgepressten rLFT CF-PEEK und die anschließende Konstruktion von Bauteilen aus diesem Material erforderlich sind. Nach der Analyse dieser Werte wurde festgestellt, dass rLFT CF-PEEK mit hochfesten Aluminium- und Magnesiumlegierungen vergleichbar ist und aufgrund seiner geringen Dichte ein Potenzial zur Gewichtseinsparung bietet, wenn diese Legierungen ersetzt werden.

Abstract

This master's thesis aims to characterize the recycled long fibre thermoplastic (rLFT) material made from carbon fibre reinforced polyether-ether-ketone (CF-PEEK), that results from the compression moulding portion of a closed loop recycling process for thermoplastic composites. The waste and offcuts generated by a thermoplastic automatic fibre placement process with in-situ consolidation, together with waste from the manufacture of the unidirectional CF-PEEK tapes needed for it, are cut to the required fibre length and are compression moulded under vacuum into the desired shape. Through flexural testing, the parameter space of the process is analysed and an optimal set of process parameters found. Fifteen plates were compression moulded from CF-PEEK chips for the material characterization, including plates of varying thicknesses and one plate processed without vacuum. Using seven different mechanical tests, six basic strengths and five engineering constants, required to model the compression moulded rLFT CF-PEEK and subsequently design parts from it, were determined. After analysing these, the rLFT CF-PEEK was found to be comparable to high strength aluminium and magnesium alloys and also have weight saving potential when replacing these alloys due to its low density.

Contents

Aufgabenstellung	III
Ehrenwörtliche Erklärung	IV
Übersicht	V
Abstract	VI
Contents	VII
Nomenclature	IX
List of abbreviations	XII
List of Figures	XIII
List of Tables	XV
1 Introduction	1
2 State of the art	3
2.1 Recycling of carbon fibre reinforced polymers	3
2.2 Compression moulding of thermoplastic composites	5
2.3 Overview of mechanical strength by other publications.....	6
3 Methods	8
3.1 Material	8
3.1.1 CF-PEEK in the form of UD tape	8
3.1.2 Characteristics of rLFT.....	11
3.2 Compression moulding	13
3.3 Testing methodology	21
3.3.1 Tensile testing.....	22
3.3.2 Compression testing	24
3.3.3 Flexural testing	25
3.3.4 Shear testing	28
3.3.5 Compression Shear testing	30
3.3.6 Plain-pin bearing test.....	32

3.4	Design of Experiment.....	35
4	Results	37
4.1	rLFT CF-PEEK after compression moulding.....	37
4.2	Optimal Parameters	39
4.3	Influence of cross-sectional thickness	46
4.4	Tensile testing.....	48
4.5	Compression testing	49
4.6	Flexural testing	53
4.7	Shear testing	53
	4.7.1 In-plane shear.....	54
	4.7.2 Interlaminar shear testing.....	55
4.8	Plain-pin bearing strength testing.....	57
4.9	Influence of vacuum during processing	60
4.10	Overview of the results.....	60
5	Discussion	62
5.1	Comparison to other publications.....	62
5.2	Comparison with other lightweight materials	65
5.3	Process considerations.....	67
6	Summary and Outlook.....	69
6.1	Summary	69
6.2	Outlook.....	70
7	Appendix.....	71
8	References.....	Error! Bookmark not defined.

Nomenclature

Symbol	Unit	Description
A_{PL}	$[cm^2]$	Plate surface area
A_{PR}	$[cm^2]$	Surface area of hydraulic cylinder
B_1	$[-]$	Percent bending around 1-axis
B_2	$[-]$	Percent bending around 2-axis
$CL95\%$		95% confidence level
E_c	$[GPa]$	Elastic modulus in compression
E_f	$[GPa]$	Flexural modulus
E_t	$[GPa]$	Elastic modulus in tension
F	$[N]$	Force
F_c	$[N]$	Compressive force
G	$[GPa]$	Shear modulus
G_{12}	$[GPa]$	In-plane shear modulus
$G_{13} = G_{23}$	$[GPa]$	Interlaminar shear modulus
L	$[mm]$	Outer span (ISO 14125 flexural test)
L'	$[mm]$	Inner span (ISO 14125 flexural test)
m_f	$[g]$	Fibre mass
m_m	$[g]$	Matrix mass
m_{PL}	$[g]$	Plate mass
p_{off}	$[bar]$	Offset pressure
p_{PL}	$[bar]$	Average compaction pressure
p_{PR}	$[bar]$	Hydraulic pressure of the press
$p_{PR,HD}$	$[bar]$	Hydraulic pressure of the press in high pressure mode

X Nomenclature

Symbol	Unit	Description
$p_{PR,ND}$	[<i>bar</i>]	Hydraulic pressure of the press in low pressure mode
$R_{p,0,2\%}$	[<i>MPa</i>]	Yield stress
t	[<i>mm</i>]	Plate thickness
T_g	[°C]	Glass transition temperature
T_{press}	[°C]	Process temperature
t_{press}	[<i>min</i>]	Pressing time
V	[<i>mm/min</i>]	Test speed
V_c	[<i>cm</i> ³]	Volume of the composite
V_f	[<i>cm</i> ³]	Volume of the fibre
w_M	[<i>wt.-%</i>]	Mass fraction of the matrix
w_F	[<i>wt.-%</i>]	Mass fraction of the fibres
γ_{12}	[–]	Engineering shear strain
ϵ_1	[–]	Engineering strain in loading direction
ϵ_2	[–]	Transverse engineering strain
ϵ_f	[–]	Flexural Strain
ν	[–]	Poisson's ratio
$\nu_{12,c}$	[–]	Poisson's ratio in compression
$\nu_{12,t}$	[–]	Poisson's ratio in tension
ρ	[<i>g/cm</i> ³]	Density
ρ_C	[<i>g/cm</i> ³]	Composite density
ρ_F	[<i>g/cm</i> ³]	Fibre density
ρ_M	[<i>g/cm</i> ³]	Matrix density
σ_c	[<i>MPa</i>]	Compressive stress

Symbol	Unit	Description
$\sigma_{m,c}$	[MPa]	Compressive strength
$\sigma_{m,c}/\rho$	[Nm/g]	Specific compressive strength
σ_f	[MPa]	Flexural stress
$\sigma_{m,f}$	[MPa]	Flexural strength
$\sigma_{m,f}/\rho$	[Nm/g]	Specific flexural strength
σ_p	[MPa]	Plain-pin bearing stress
$\sigma_{m,p}$	[MPa]	Plain-pin bearing strength
σ_t	[MPa]	Tensile stress
$\sigma_{m,t}$	[MPa]	Tensile strength
$\sigma_{m,t}/\rho$	[Nm/g]	Specific tensile strength
τ_m	[MPa]	Shear strength
τ_m/ρ	[Nm/g]	Specific shear strength
τ_{12}	[MPa]	In-plane shear stress
$\tau_{m,12}$	[MPa]	In-plane shear strength
$\tau_{13} = \tau_{23}$	[MPa]	Apparent interlaminar shear stress
$\tau_{m,13} = \tau_{m,23}$	[MPa]	Apparent interlaminar shear strength
φ_F	[vol.-%]	Fibre volume content
φ_M	[vol.-%]	Volume content of the matrix

List of abbreviations

Abbreviation	Description
AFP	Automated fibre placement
BMC	Bulk moulding compound
CF-PEEK	Carbon fibre reinforced polyether-ether-ketone
CFRP	Carbon fibre reinforced plastic
CFRTP	Carbon fibre reinforced thermoplastic
CLC	Combined loading compression
CTE	Coefficient of thermal expansion
DIC	Digital image correlation
DoE	Design of experiment
FVC	Fibre volume content
HD	High pressure (Hochdruck)
ILS	Interlaminar shear
ISO	International organisation for standardization
LCC	Chair of Carbon Composites (Lehrstuhl für Carbon Composites)
ND	Low pressure (Niederdruck)
PCCL	Polymer Competence Center Leoben GmbH
QI	Quasi-isotropic
PEEK	Polyether-ether-ketone
RSM	Response surface modelling
rLFT	Recycled long fibre reinforced thermoplastic
SG	Strain gauge
TP-AFP	Thermoplastic automated fibre placement
UD	Unidirectional

List of Figures

Figure 3-1 CF-PEEK tape scraps that serve as basis for the recycling process.....	10
Figure 3-2 Axes definition for fibre-reinforced plastic composite [14]	11
Figure 3-3 12x12mm chips placed in the mould cavity prior to compression moulding	12
Figure 3-4 The 100-ton laboratory press with mould placed inside	13
Figure 3-5 Mould installed in hydraulic press	15
Figure 3-6 Lower mould half with wedge inserts installed, top view	15
Figure 3-7 Distance blocks for 20mm, 10mm, 6mm and 4mm thick plates.....	15
Figure 3-8 Thermocouple positions projected on top surface of a plate	17
Figure 3-9 Process diagram (not to scale)	17
Figure 3-10 Flowchart of the compression moulding process.....	19
Figure 3-11 Type 1B sample according to ISO 527 with axes definition	22
Figure 3-12 CLC sample with strain gauges applied to both sides	25
Figure 3-13 4-point flexure test setup.....	26
Figure 3-14 Sample for V-notched rail shear test with axes definition	29
Figure 3-15 Schematic diagram of the compression shear test	31
Figure 3-16 Test setup for plain-pin bearing strength according to ISO 12815 [29]	33
Figure 3-17 Test jig for ISO 12815 plain pin bearing strength test.....	34
Figure 4-1 Cross section of 4,48mm thick quasi-isotropic compression moulded laminate with a $(0^{\circ}/-45^{\circ}/90^{\circ}/+45^{\circ})_{8S}$ stacking sequence at 5x magnification.....	38
Figure 4-2 Cross section of 2mm thick rLFT CF-PEEK plate at 5x magnification	38
Figure 4-3 Cross section of 4mm thick rLFT CF-PEEK plate at 5x magnification	38
Figure 4-4 Cross section of 6mm thick rLFT CF-PEEK plate at 5x magnification	38
Figure 4-5 Cross section of 10mm thick rLFT CF-PEEK plate 5x magnification.....	38
Figure 4-6 Summary of flexural strengths for the DoE statistical modelling.....	40
Figure 4-7 Summary of flexural moduli for the DoE statistical modelling.....	41
Figure 4-8 Summary of fit for the statistical model from MODDE	43
Figure 4-9 Response contour plot of the flexural strength from MODDE.....	44
Figure 4-10 Response contour plot of flexural strength variability as a fraction of flexural strength, from MODDE.....	45

Figure 4-11 Flexural strength of 2mm, 4mm 6mm and 10mm thick rLFT CF-PEEK ...	46
Figure 4-12 Flexural modulus of 2mm, 4mm 6mm and 10mm thick rLFT CF-PEEK ..	47
Figure 4-13 Type 1B tensile samples for testing according to ISO 527	49
Figure 4-14 Combined loading compression fixture with a sample installed, after testing, strain gauge wires already removed	50
Figure 4-15 Axial and transvers strains from CLC sample number P4806 with double sided application of strain gauges (SG).....	52
Figure 4-16 Cross section of CLC sample number P4805 after testing at 5x magnification.....	53
Figure 4-17 In-plane shear sample mounted in the V-notched rail shear test jig.....	54
Figure 4-18 V-notched rail shear sample with the area used for measuring shear strain indicated by a red rectangle.....	55
Figure 4-19 Failure modes of ISO 14130 samples: a) partial interlaminar crack from left side towards middle, tensile break; b) plastic deformation and partial layer separation; c) pure tensile break of the bottom most layer	56
Figure 4-20 Two samples for the determination of ILS strength using compression shear testing, after testing	57
Figure 4-21 Plain pin bearing strength sample P4801 after testing	58
Figure 4-22 Plain pin bearing strength sample P4809 tested beyond its yield point: Left – complete sample; Right – close up of tested area	58
Figure 4-23 Force diagram of samples P4806 and P4809 during plain-pin bearing testing	59
Figure 7-1 Coefficient plot of the statistical model from MODDE	72

List of Tables

Table 3.1 Unidirectional CF-PEEK Material properties	9
Table 3.2 Parameters hydraulic press	14
Table 3.3 Weight of rLFT CF-PEEK needed for plates of varying thicknesses	20
Table 3.4 Symbols used for strengths and engineering constants	21
Table 3.5 Summary of parameters for flexural testing	27
Table 3.6 Test plan for the DoE test series	36
Table 4.1 Overview of strengths and engineering constants for 4mm samples of 12x12mm rLFT pressed at 395°C and 110 bar	61
Table 5.1 Material properties of 4mm rLFT CF-PEEK with 12x12mm chips pressed at 395°C and 110 bar, MC1200 PEEK BMC and MS-4H Epoxy BMC [15]	63
Table 5.2 Relative comparison of 12x12mm rLFT pressed at 395°C and 110 bar and the UD tape it is made from.....	64
Table 5.3 Material properties of 7075 T6 and 6061 T6 aluminium alloys [15,34], 4mm rLFT CF-PEEK with 12x12mm chips pressed at 395°C and 110 bar and AZ80A T5 magnesium alloy [34].....	65
Table 7.1 Flexural strengths and moduli of experiments from the DoE test series	71

1 Introduction

The use of carbon fibre reinforced polymers (CFRP) increases in volume year over year, especially as prices go down and this lightweight and high strength material becomes more affordable for applications other than aerospace. This growth necessitates the development of methods to recycle CFRPs not only because of the larger volume generated, but because the production of carbon fibres is a very energy intensive process.

In recent decades the thermoset matrices, that are traditionally used for the production of CFRPs, have been slowly giving way to thermoplastics. This is primarily because of the ability of thermoplastics to be melted and shaped more than once. In contrast, the shape of a CFRP part with a thermoset matrix is fixed, once the cross-linking reactions of the curing process have taken place. This in turn means that the recycling of thermoset CFRPs requires the separation of matrix and fibre, which is generally achieved by destroying the thermoset matrix. Carbon fibre reinforced thermoplastics (CFRTPs), such as the carbon fibre reinforced polyether-ether-ketone (CF-PEEK) used in this thesis, on the other hand can be heated up above their melting temperature and brought into a different shape. One way to achieve that is to reduce the CF-PEEK scraps to a certain uniform size and use a compression moulding process, that applies temperature and pressure in a mould, to form the material into the desired shape. Since this master's thesis is a part of the REUSELAGE project, the compression moulding is just one step in a closed loop process, that aims to use scraps generated during an automated fibre placement process with in-situ consolidation for thermoplastic composites (TP-AFP). These scraps, together with waste generated during the manufacture of the UD CF-PEEK tapes needed for TP-AFP, are chopped to a uniform size and compression moulded, at which point the parts can be used as is or fed back into the TP-AFP process to create integrally built structures. The aim of this master's thesis is to analyse the mechanical properties of the recycled long fibre thermoplastic carbon fibre polyether-ether-ketone (rLFT CF-PEEK) material that results from a vacuum assisted compression moulding process. The influences that part thickness and processing in air rather than in vacuum have on the mechanical strength of the

2 Introduction

material will also be explored. Additionally, the study of the parameter space of the compression moulding process, that was not concluded in my term project preceding this master's thesis, will be finished and the results from it presented.

This master's thesis will present the current state of the art in the field of recycling CFRPs, compression moulding and mechanical testing of rLFT CF-PEEK, the methods used for both the compression moulding process and the mechanical testing, as well as the results and knowledge gathered. Lastly, the material properties of the rLFT CF-PEEK will be discussed in the context of other publications for the same material, as well as other lightweight materials.

2 State of the art

In this chapter, the current state of research regarding recycling of carbon fibres, compression moulding and mechanical testing of rLFT CF-PEEK will be presented.

2.1 Recycling of carbon fibre reinforced polymers

The recycling of CFRPs is necessitated not only by end-of-life parts, but waste generated during production, as its volume can be up 20% of the weight of the finished part. Vincent in [1] gives an example in Figure 1.1 of some of the places where waste is generated during the manufacturing process, such as prepreg impregnation, nesting of parts on a sheet, trimming edges and part rejection. Depending on the type of process used, the carbon fibres can be dry or pre-impregnated with matrix, the latter of which necessitates either immediate processing or curing the resin, if the prepreg has thermoset matrix. Once the thermoset matrix is set, the only way for recycling is to separate the matrix and fibres.

The most common method of matrix removal from the carbon fibres is called pyrolysis. Lopez-Uriónabarrenechea et al. explore the process in [2], which utilizes temperatures of between 400°C and 600°C and a lack of oxygen to breakdown the matrix into gases and vapours. This process leaves some carbon residue on the fibres, which can be burned off in a controlled manner or chemically stripped. These reclaimed fibres are coated with sizing and are ready to be used again. The pyrolysis process can also be done using microwaves, which selectively heats only the fibres, as Seiler et al. shows in [3]. The microwaves induce currents in the carbon fibres because they are conductive, while the matrix is a dielectric and not only does not get heated by the microwaves, but also does not prevent the electromagnetic energy from reaching the fibres. The major advantage of this approach is the short process time and low energy consumption. The author found that 4,5 to 5 minutes at 900W power of a 2,45GHz microwave source is enough to heat up the 40g to 60g of material they tested to between 500°C and 550°C.

The electrical conductivity of carbon fibres has also been utilized by Roux et al. [4]. The electrodynamic fragmentation works by applying very high voltage pulses, 180 kV in this study, to a CFRP part, a door hinge in the case of this particular study. The high voltage creates a plasma channel in the part, which is very hot and also very concentrated. This causes some of the carbon fibres in the plasma channel to sublime and the PEEK matrix to pyrolyze. These gasses expand between the layers of the part and cause mechanical delamination, while the pressure waves from the process propagate throughout the material and weaken it. The authors then compression moulded the fragmented pieces into the same door hinge, tested it and found a 17% reduction in strength compared to hinge made from virgin material.

From the processes presented so far, pyrolysis is the only process for extracting carbon fibres from CFRPs, that is done on an industrial scale. Solvolysis is the second such process and it uses chemicals to breakdown the matrix of CFRPs [5]. The authors of [5], Morin et. al, examine the solvolysis process for breaking down epoxy and phenolic resins using pure water, alcohols or acetone at a supercritical state. At pressures between 22,1 MPa and 35 MPa, as well as temperatures between 400°C and 600°C, the fluid used behaves both like a fluid and gas, which allows it to strip between 95% and 100% of the matrix from the carbon fibres. Other types of solvolysis take place at low temperatures, utilizes water, alcohol, glycol and others for solvents and has the benefit of not breaking down the monomers of epoxy and phenolic resins, making it possible to recover those [5].

The repurposing of carbon fibre waste does not have to involve separating matrix and fibre, when the former is a thermoplastic. This is economically desirable because no new matrix is required for the recycling, which is especially important when it comes to high performance composites such as CF-PEEK, where the matrix forms a significant part of the composite cost. CFRTP waste can be heated up to a state, where the matrix is malleable and can be reshaped into a useable part. One way to achieve this is to chop up the CFRP to fibre lengths of about one millimetre, which allows the material to be injection moulded, either as is or through the addition of more matrix. Such short fibre reinforced thermoplastics are very easy to produce, since they can utilize existing injection moulding equipment and process knowledge, but their strength is much lower than that of continuous fibre reinforcement. Compression moulding using long fibre

reinforcement is a method for recycling thermoplastic composites, that strikes a balance between ease of processing and mechanical strength.

2.2 Compression moulding of thermoplastic composites

Compression moulding turns scraps or chips of thermoplastic composites into a discontinuously reinforced material, which is called long fibre thermoplastic or LFT. The definition of what long fibre reinforcement is varies between sources, with most sources citing a minimal fibre length of 1mm to 10mm [6–8] and maximal length of 25mm to 50mm [7,9]. [1] gives another criterion for long fibres: L/d over 1000, which means fibres longer than 6mm, assuming a typical fibre has a diameter of $6\mu\text{m}$.

The sequence of the compression moulding process is illustrated in Figure 1 of the publication by Selezneva and Lessard [10]. The thermoplastic composite is cut, shredded or hammer milled into pieces (chips), placed in the mould and formed by heating it above the melting temperature of the polymer and applying the compaction pressure. Because the CF-PEEK chips occupy between four and eight times the volume of the finished LFT part, a debulking step, consisting of compressing the chips in the mould with pressure similar to the compaction pressure used later on in the process, is sometimes used [11]. Several publications, as well as material datasheets give sets of process parameters with which to compression mould CF-PEEK. Selezneva and Lessard in [10] create their plates using a debulking step and a 380°C compaction temperature at which the process dwells for 15 minutes with 35 bar of pressure applied, after which the material is cooled at $10^\circ\text{C}/\text{min}$. DeWayne and Fukumoto in [12] suggest applying 34 bar for the debulking step and recommends pressure between 34 bar and 69 bar for the consolidation step with a zero to two minutes dwell period at 385°C . The recommended cooling rate is between $5^\circ\text{C}/\text{min}$ and $20^\circ\text{C}/\text{min}$ with $0,5^\circ\text{C}/\text{min}$ cooling rate allowing the PEEK polymer to achieve 43% crystallinity and $20^\circ\text{C}/\text{min}$ resulting in 25% crystallinity. DeWayne and Fukumoto use a CF-PEEK bulk moulding compound (BMC) MC1200 made by Toray Advanced Composites for their experiments, which recommends in its datasheet the same process parameters as the publication. Li and Englund [13] do a study of the process parameters with three temperatures and four dwell periods, using between 34 bar and 41 bar of compaction pressure. The authors conclude that 390°C and 16 minutes are the

optimal parameters for their process. All publications require the compaction pressure to be applied until the material is cooled below its glass transition temperature of 143°C.

Only one publication was found, that utilises vacuum when compression moulding. Tapper et al. conduct the compression moulding in [14] under vacuum to prevent the degradation of the polypropylene matrix in their composite material. No references to vacuum assisted compression moulding processes with the goal of reducing void content were found while researching the topic, or using vacuum to prevent the degradation of PEEK matrix at high temperatures.

2.3 Overview of mechanical strength by other publications

A study done by Selezneva and Lessard [10] is the most comprehensive and relevant to the topic of this master's thesis. In it, the authors use CF-PEEK tape with a thickness of 0,14mm and fibre volume content (FVC) of 60% to manufacture 2,5mm and 6mm thick plates for their specimen. The Tenax[®]-E TPUD PEEK-HTS45 material to be used in this master's thesis is very similar with tape thickness of 0,14mm and FVC of 58,8%. The authors used 8 chip sizes with varying widths and lengths, but always rectangular with the fibre length bigger than the width of the chip. From these, 8 samples for each of the tensile, compression and in-plane shear tests were cut. The tests were conducted according to the ASTM D3039, D3410 and D7078 standards respectively. All strain measurements were done using a digital image correlation system and area averaging of the strains. All results in the study were normalized with values from a quasi-isotropic laminate (QI) with a $(0^\circ/\pm 60^\circ)_{3S}$ lay-up and no absolute values for all the strengths or moduli were published. The tensile modulus of all 8 plates with different chip sizes was found to be between 70% and 80% that of the QI laminate, while the tensile strengths were all under 60% the reference value. The compression strength is between 45% and 90%, while the compression modulus is between 60% and 100% that of the QI laminate. The in-plane shear test shows similar relative shear strength and shear modulus as the compressive test. The authors of the study also quantified the warping of the rLFT plates, that they observed.

As mentioned previously, DeWayne and Fukumoto use the MC1200 BMC with 25,4mm long fibres, for which the manufacturer provides tensile, compressive and flexural strengths and moduli in the material datasheet [11]. The tensile strength is 288,9 MPa, the compressive strength is 312,3 MPa and the flexural one is 657,8 MPa with 43,4 GPa, 48,3 GPa and 40 GPa being the respective moduli. Another BMC by the same manufacturer, that uses the same type of fibre and fibre length as the MC1200, but an epoxy matrix is the MS-4H [15]. Even though it is not a CF-PEEK composite, the datasheet of that particular BMC provides approximate values for the shear strength, shear modulus and bearing strength, that can be expected from a long fibre reinforced polymer. Those are 177,9 MPa, 12,4 GPa and 858,4 MPa respectively.

The two publications above both use UD tape, that is slit and chopped into the desired size. While this tight control over the size of chips is very beneficial to scientific research, it is not how the recycling process would function on an industrial scale. Li and Englund adopt in their publication [13] a process for creating the chips need for the compression moulding process, that is more suitable for high-volume production. The authors hammer mill and/or shred their source material, followed by sieving to separate the chips into 5 different sizes. These different sized chips alone, as well as combination from different sizes in varying ratios, were compression moulded and 5 samples for each of the two tests – flexural and tensile cut out. For the 12,7mm chip size, the authors obtained tensile strength of around 50 MPa with tensile modulus of roughly 20 GPa, while the flexural strength and modulus are about 200 MPa and 15 GPa.

The Tenax[®]-E TPUD PEEK-HTS45 material [16], that will be used in this master's thesis, has in its UD tape form a tensile strength of 2270 MPa, compressive strength of 1545 MPa and a flexural one of 1760 MPa. The respective moduli are 141 GPa, 130 GPa and 130 GPa.

3 Methods

In the following chapter the manufacturing and testing methodologies used during this master's thesis will be presented. This includes the material, the compression moulding equipment, the press process itself and the mechanical tests needed for the material characterization. Lastly, a brief overview of the test series for the determination of the optimal process parameters will be given, as it is a continuation of my term project and will be concluded as part of this master's thesis.

3.1 Material

The properties of the CF-PEEK material before it is compression moulded will be discussed below, as well as the material behaviour of rLFT.

3.1.1 CF-PEEK in the form of UD tape

As explained in Chapter 2.3.3, the TP-AFP process uses pre-impregnated tapes of PEEK with unidirectional continuous carbon fibre reinforcement along the length of the tape. These tapes come in the form of rolls from the manufacturer and get fed into the AFP machine. In the course of this master's thesis the Tenax[®]-E TPUD PEEK-2-34-HTS45 P12 12K-UD-145 [16] made by Teijin Europe GmbH will be used. This material consists of Tenax[®]-E HTS45 with a filament count of 12000 to a yarn and a proprietary sizing, developed especially for the thermoplastic matrix - a polyether-ether-ketone. The HTS45 12K yarn has on its own a tensile strength of 4500 MPa, an elastic modulus of 240 GPa and a density of 1,77 g/cm³ [17]. The prepreg UD tape with a 34 wt.-% matrix content has a tensile strength of 2270 MPa, an elastic modulus of 141 GPa [16] and an average density of 1,58 g/cm³. The density of the prepreg is not given by the manufacturer, but can be calculated with the help of the information in the datasheet [16], Equation 3-1 and Equation 3-2.

$$\rho_c = \varphi_f \rho_f + \varphi_m \rho_m \quad (3-1)$$

$$\varphi_f = \frac{V_f}{V_c} = \frac{m_f / \rho_f}{\frac{m_f}{\rho_f} + \frac{m_m}{\rho_m}} = \frac{1}{1 + \frac{\rho_f}{\rho_m} * \frac{w_m}{1 - w_m}} \quad (3-2)$$

Table 3.1 Unidirectional CF-PEEK Material properties

T_g	ρ_M	ρ_F	ρ_C	w_M	w_F	φ_M	φ_F
143	1,3	1,77	1,5763	34	66	41,22	58,78
[°C]	[g/cm ³]	[g/cm ³]	[g/cm ³]	[wt.-%]	[wt.-%]	[vol.-%]	[vol.-%]

The manufacturer provided the LCC with both 304.8mm wide rolls of the material, that failed quality control, and also scraps generated during the production process. These scraps, shown in Figure 3-1, have a length of between 20mm and 80mm and a width of between 6mm and 30mm, with the carbon fibre reinforcement oriented along the length of these scraps. These big variations in the dimensions of the production scraps are undesirable, because of the major influence the fibre length has on the mechanical properties of LFT materials [6]. In order to reduce or eliminate the influence of the parameter fibre length on the mechanical properties, so that changes in the mechanical properties of the different plates can be attributed more directly to changes in other factors, it is necessary for the material that is put into the mould to have a very small variation in the fibre length from one chip to another. This can be achieved through either putting the production scraps through a shredder or cutting uniform chips from the 304.8mm wide roll of material. The latter option is more feasible for the limited number of experiments needed for this master's thesis due the availability of a M1200 cutting plotter made by Zünd AG. With it, different sizes of chips with very little variance in their width and length can be created, something a shredder is unable to do. While using a cutting plotter does have its advantage for scientific purposes, it has to be said that for a production run, this method is very slow, it consumes cutting blades and is not a prerequisite to ensure good part quality. A shredder is better suited for manufacturing and would be an adequate way of cutting the source material into chips, if it is able to provide a small enough fibre length distribution as to not cause significant variations in the quality of the parts.



Figure 3-1 CF-PEEK tape scraps that serve as basis for the recycling process

With the method of producing the required chips settled on, the next step is to determine the shape and size of the chips. These decisions were analysed in depth in my term project [18], that precedes this master's thesis. Due to the low strength of a unidirectional lamina perpendicular to the fibre axis, the tapes have a tendency to split between the fibres very easily, so it was decided to use rectangular chips with the fibres oriented parallel to the longer side of the rectangle. Rectangular chips were also used in [10,12,19,20], so using such chips allows to compare results. Further, a square shape was settled upon in order to avoid a preference in the chip orientation and by extension the fibre orientation when filling the mould with chips. This should prevent the chips from interlocking, getting tangled in one another or bundling, which from practical experience happens increasingly often with chips that have high aspect ratios, and causes a less random orientation of the fibres in a given area of a part. Lastly, the sizes of the chips used in the term project are 6x6mm, 12x12mm and 18x18mm and these sizes will be used here as well.

The CF-PEEK provided by Teijin Europe GmbH and to be used in this master's thesis is virgin material, meaning that both the tape and the production scraps have not yet been processed, outside of their manufacture. This is important, because the PEEK polymer degrades when it is heated above its melting temperature [21], especially if the processing takes place in an oxidizing environment. In [21], the authors conclude, that holding the PEEK in its molten state also impedes its ability to crystallize. This in turn leads to lower strength of the matrix. These two phenomena limit the practical number of times the CF-

PEEK can be recycled. Another degradation of the mechanical properties with each subsequent recycling could come from shortening of the fibres in the composite material, when rLFT parts are being chopped up to the size needed for processing. The effect fibre length has on the mechanical properties has been studied in [10,19]

3.1.2 Characteristics of rLFT

In this master's thesis, the recycled long fibre reinforced thermoplastic is created from unidirectionally reinforced chips of PEEK, that are placed in a mould cavity with random fibre orientation in the 12-plane and fibre axes parallel to said 12-plane, as shown in Figure 3-3. The 12-plane is defined as being parallel to the lower surface of the mould cavity, while the 3-axis coincides with the thickness direction of the plate, as can be seen in Figure 3-2. This arrangement of chips results in quasi-isotropic layers of CF-PEEK stacked on top of each other with the 12-plane being the one exhibiting the quasi-isotropic property. Perpendicular to the 12-plane and along the 3-axis, these individual layers behave like a UD lamina along its thickness in that they both exhibit transverse fibre properties. This means that the rLFT plate behaves along the 3-axis similarly to a unidirectionally reinforced laminate, with the exception of layer undulations, that will be discussed in Chapter 4.1. This description of the material behaviour is valid only for the plate geometry tested here and may not be true for more complex parts.

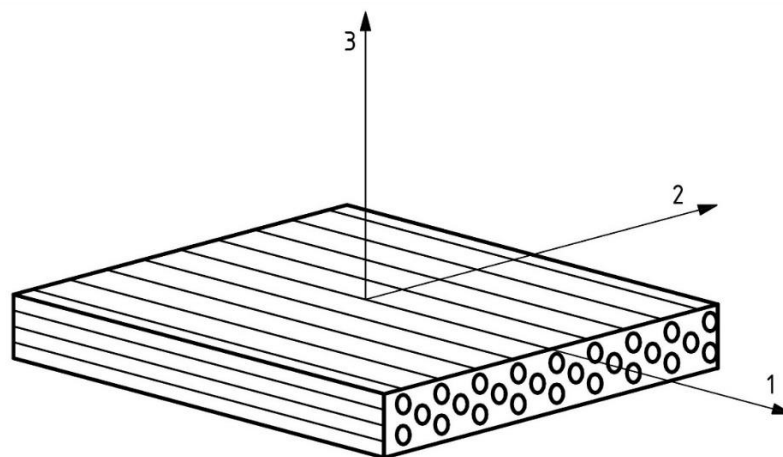


Figure 3-2 Axes definition for fibre-reinforced plastic composite [14]

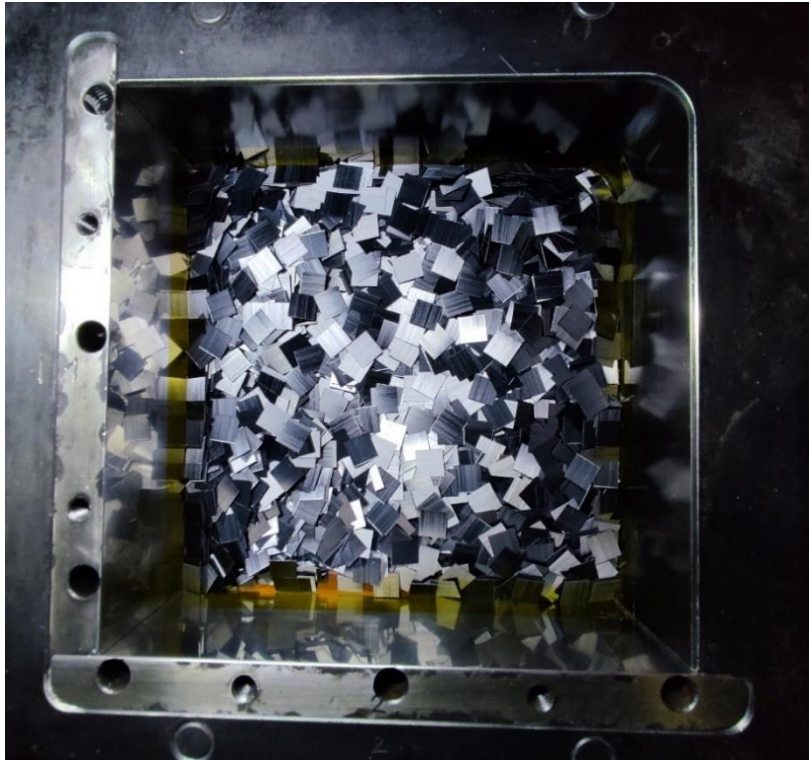


Figure 3-3 12x12mm chips placed in the mould cavity prior to compression moulding

Another important aspect of the long fibre reinforcement is the high number of fibre ends that exist within the finished part. These free ends cause localised stress concentrations on the microscopic level due to the mismatch between the longitudinal modulus of elasticity of the carbon fibre and the modulus of elasticity of the PEEK polymer. These stress concentrations lead to easier failure of the fibre-matrix interface and subsequently the part as a whole.

One of the benefits of compression moulding is its ability to quickly and efficiently produce complex geometries. One problem that arises from such geometries is the complicated stress field that cannot be modelled easily, especially when the material behaves anisotropic on the whole. In such cases, a complete characterization of the material properties is needed in order to allow the correct modelling for design and evaluation purposes. One material parameter often overlooked in publications, but very relevant for material modelling, is the Poisson's ratio. This is why this master's thesis will determine the Poisson's ratio, while conducting both the tensile and compression testing. It should be noted, that a strong variation in the Poisson's ratio of the tested samples is possible, since the orientation and placement of the chips is not being controlled for here, as stated before. Consequently, the laminate structure of not only

different plates, but even different areas of the same plate can vary, leading to different amounts of fibres being oriented along the 1- or 2-direction of the specimens. That fibre orientation is what primarily determines the mechanical behaviour and properties.

3.2 Compression moulding

The compression moulding process takes the CF-PEEK chips and through the application of heat and pressure in a confined space compresses them into the desired shape. This master's thesis uses a combination of a laboratory hydraulic press and a purpose made mould to process the CF-PEEK material.

The laboratory hydraulic press used in this master's thesis can be seen in Figure 3-4. It is capable of exerting 100-ton of force, heating the work plates up to 500°C and, using a combination of compressed air and water, also cool the work plates. The most important feature of the press is the enclosed work volume, which is designed to be placed under vacuum using the built-in vacuum pump.



Figure 3-4 The 100-ton laboratory press with mould placed inside

The force of the press is controlled by varying the hydraulic pressure. Since the applied force will also be expressed in pressure later in this thesis, Equation 3-3 thru Equation 3-5 are used to calculate the pressure applied by the hydraulic system p_{PR} needed to achieve a certain average pressure p_{PL} on the CF-PEEK material. In order to achieve better resolution at lower forces, the press has a low pressure (ND) operating mode, which works by applying the same hydraulic pressure as in high pressure (HD) mode, but to a smaller surface area $A_{PR,ND}$ of the same lifting cylinder. Due to the lower working plate being the one that moves, a certain amount of pressure is needed to lift it, as well as the mould, so a pressure offset p_{off} needs to be added.

$$p_{PR} = p_{off} + \frac{A_{PL}}{A_{PR}} p_{PL} \text{ [bar]} \quad (3-3)$$

$$p_{PR,ND} = 25 + 7,95 \times p_{PL} \text{ [bar]} \quad (3-4)$$

$$p_{PR,HD} = 3 + 1,155 \times p_{PL} \text{ [bar]} \quad (3-5)$$

Table 3.2 Parameters hydraulic press

A_{PL}	$A_{PR,ND}$	$A_{PR,HD}$	$p_{off,ND}$	$p_{off,HD}$	$p_{PR,max}$
400	50,3	346,4	25	3	300
[cm ²]	[cm ²]	[cm ²]	[bar]	[bar]	[bar]

The second major component needed for the compression moulding process is the mould. The one used in this master's thesis was developed and manufactured by Eckerle GmbH in cooperation with the LCC. It consists of two halves, with the lower one forming a square cavity with 200mm sides and 62mm deep, while the top half forms the 60mm long punch, that fits into said cavity. The top half is guided into the lower one using four centering pins. Figure 3-5 shows the two halves installed in the hydraulic press. In order to vary the thickness of the pressed plate, four distance blocks, one on each side of the punch, are used to space the face of the punch the appropriate distance from the bottom of the cavity. The mould was delivered with sets of distance blocks, which allow the pressing of 2mm, 4mm, 6mm, 10mm, or 20mm thick plates. Figure 3-7 shows examples of the different distance blocks.

The mould itself is made from hardened tool steel, including the two wedge inserts, which can be seen in Figure 3-6. These form two of the sides of the cavity and the surfaces of the inserts opposite to those are angled at a 5° angle, so that they can be more easily removed while demoulding.

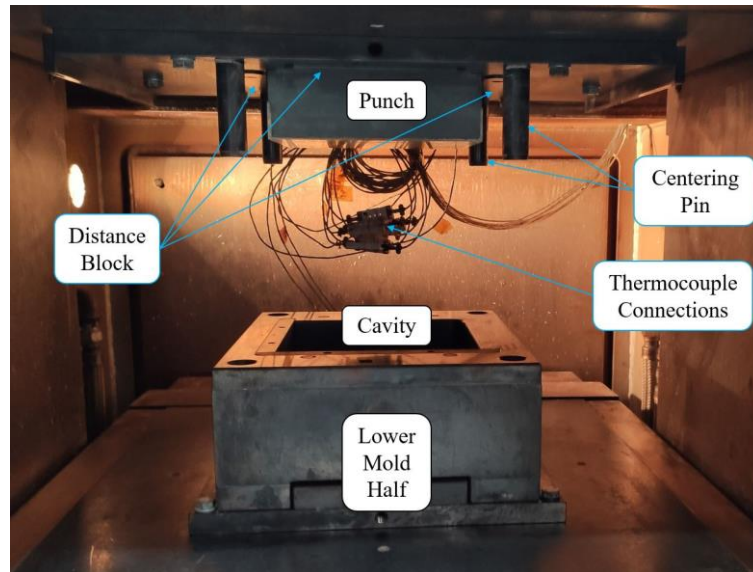


Figure 3-5 Mould installed in hydraulic press

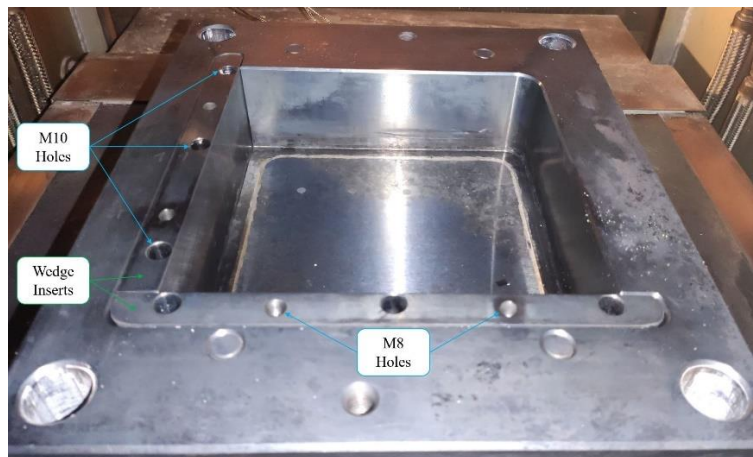


Figure 3-6 Lower mould half with wedge inserts installed, top view



Figure 3-7 Distance blocks for 20mm, 10mm, 6mm and 4mm thick plates

In order to ease the demoulding process, polyimide film of 50 μ m thickness was used on the bottom and top of each plate. This film was necessary due to problems early on in the test series of removing plates from the mould, despite using three coats of HT400+ releasing agent made by Haufler Composites GmbH [22]. While producing the plates needed for this master's thesis, the application method of the HT400+ was switched from a paper towel to a brush, which increased the effectiveness of the release agent tremendously. At this point the use of the polyimide film was likely not necessary, but was continued, so that potential problems can be avoided.

As previously mentioned, the use of vacuum while compression moulding is rare, if at all present in the scientific publications concerning the topic here. The reason vacuum is useful during compression moulding is that it has the potential to reduce the number and size of voids in the compression moulded part. Low void content has a positive effect on the mechanical strength of a part. Another reason for processing under a lack of air is that the PEEK matrix degrades when exposed to high temperatures. As stated in [21], the degradation rate increases, when the processing takes place in an oxidizing atmosphere, as the specimen there processed under air exhibited substantially longer crystallization half-times. Semi-crystallin PEEK is desirable for structural applications, because it has superior mechanical properties compared to amorphous PEEK. This is a further reason why processing the CF-PEEK chips under vacuum should contribute to higher mechanical strength and why the use of vacuum was pursued in this master's thesis.

For control and monitoring purposes, three thermocouples of the EST-73023 type made by Therma Thermofühler GmbH were installed in each mould half. Their positions are shown in Figure 3-8. TC1, TC2 and TC3 are located in the lower half, while TC4, TC5 and TC6 are in the punch. The temperatures were recorded on a laptop with the help of a TC-08 USB datalogger made by Pico Technology and used to control the compression moulding process.

As a part of my term project [18], preceding this master's thesis, an analysis of the parameters relevant for the compression moulding process was carried out and four were recognized as having a significant influence on the resulting mechanical strength. The compaction pressure p_{PL} , the pressing temperature T_{press} , the time spent at pressing temperature t_{press} and the chip size. After the first few experiments, it was decided to eliminate the pressing time t_{press} as a variable, because an effective control of it was hindered by the thermal inertia of the hydraulic press and mould combination. The

problem is explained in detail in Chapter 3.2.3 of [18]. As starting points for the rest of the parameters, values from the material datasheet [16] were used. The manufacturer recommends process parameters of $T_{press} = 390^{\circ}\text{C} \pm 10^{\circ}\text{C}$ and $p_{PL} = 20\text{bar} \pm 10\text{bar}$. The low end of this recommendation, 380°C and 10 bar, were taken as a baseline and then increased in four equal steps of 15°C and 25 bar respectively, ultimately reaching maximums of 440°C and 110 bar. The smallest chip size used here coincides with the narrowest tape the manufacturer sells – 6,35mm.

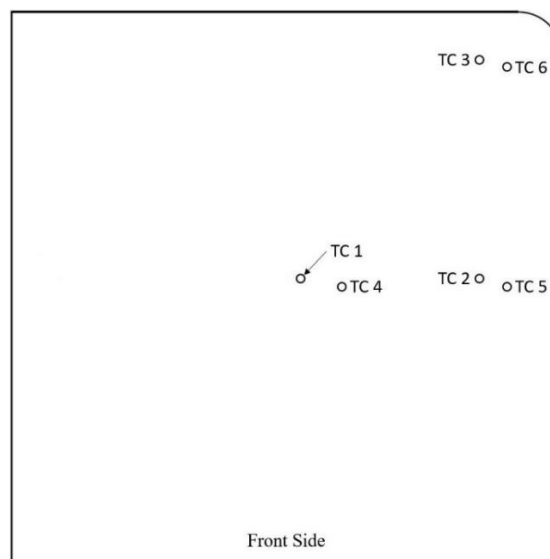


Figure 3-8 Thermocouple positions projected on top surface of a plate

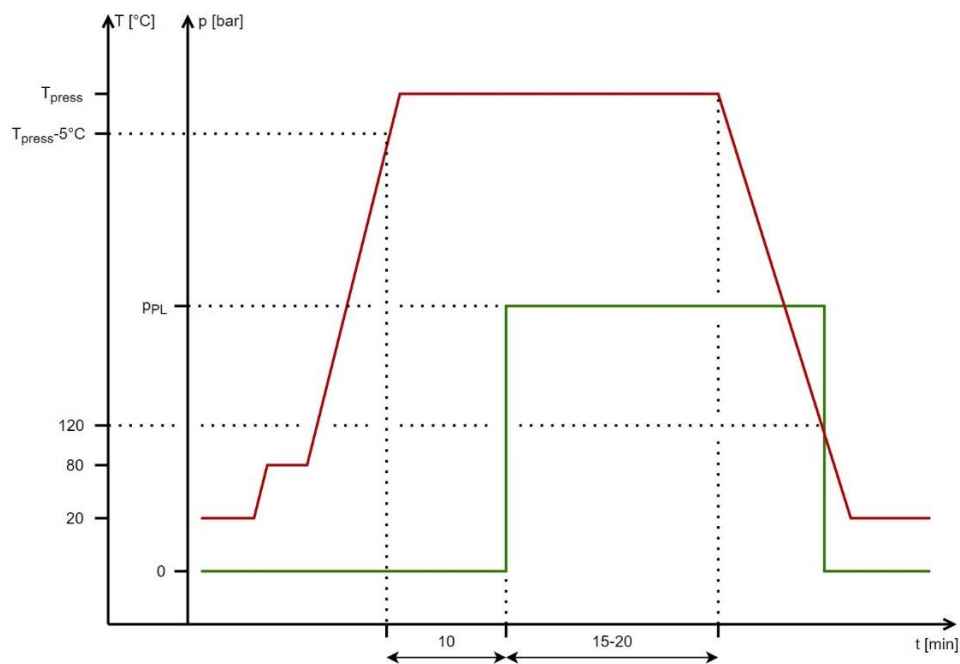


Figure 3-9 Process diagram (not to scale)

Figure 3-9 illustrates the temperature and pressure during the process, while Figure 3-10 shows the process step by step. Firstly, the mould is heated up to 80°C so that the HT400+ releasing agent can be applied. After the application is completed, the CF-PEEK chips are placed in the mould cavity and the mould is closed far enough, that the punch is just touching the top surface of the material. During experimentation it was found, that the chips occupy about 6 times the volume of the finished plate and that was used to determine the required position of the punch. This step allows the material to be evenly heated from both the top and the bottom. After this, the working volume of the press is evacuated and the heating takes place. 5°C before T_{press} is reached, the temperatures in the mould and of the material are given 10 minutes to equalize. Following that, the compacting pressure p_{PL} is applied and held until the part has been cooled below its glass transition temperature T_g . 10 minutes after p_{PL} is applied, the cooling of the hydraulic press is turned on, but due to the high thermal inertia of the system, it takes additional 5 to 10 minutes for the temperature of the CF-PEEK to start dropping. The glass transition temperature of the material used is 143°C [16], but the demoulding temperature was chosen at 120°C in order to make sure no damage due to plastic deformation can occur to the part while demoulding. The elevated temperature was chosen and not room temperature, so that an industrial process can be simulated more closely. After cooling below 120°C air is let back into the enclosure of the hydraulic press, the mould opened, the wedge inserts taken out and the plate removed, after which the process is done.

One aspect of the compression moulding process, that is not examined in detail but still very important, is the processibility. It describes how easy it is to turn the starting material into the desired shape and is dependent on how complex the geometry is. The processibility strongly depends on the fibre length [6] and its qualitative effect are depicted in Figure 5.8 of [6]. The elastic modulus, strength and impact toughness of LFT increase with increased fibre length, but processing the material gets more difficult. This can lead to features in the mould cavity not getting completely filled or the matrix and fibres separating and only the PEEK polymer flowing into said features, when the fibre length is too big for a particular feature.

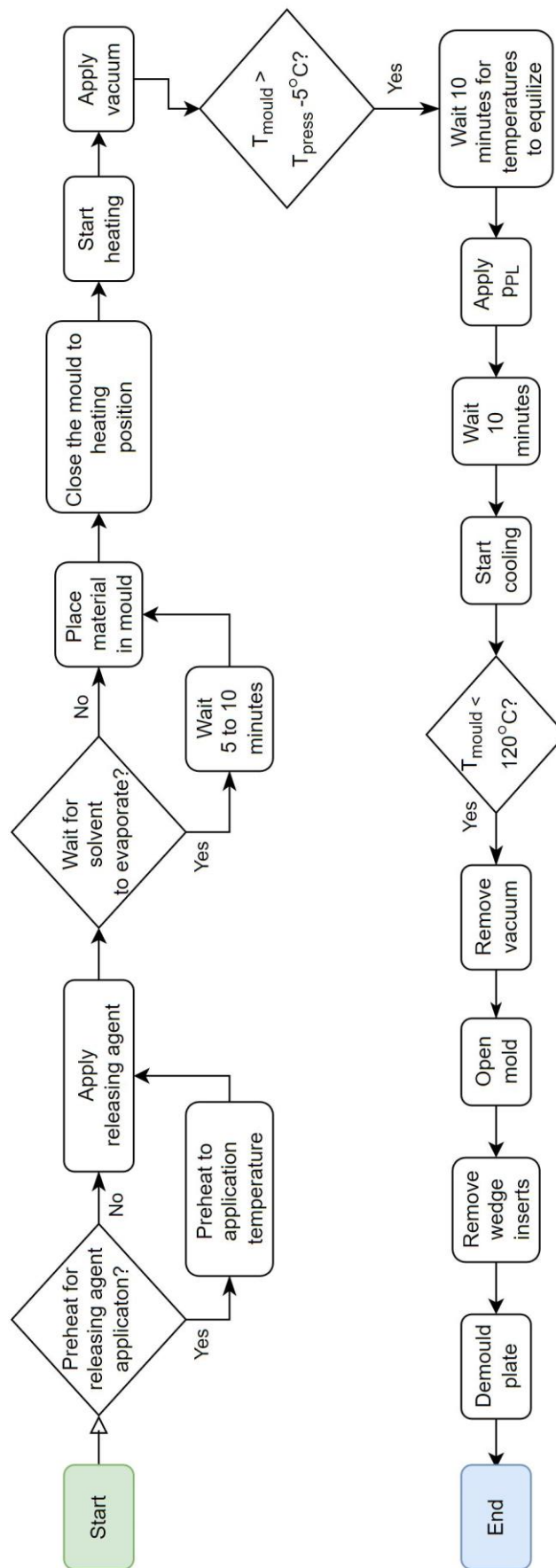


Figure 3-10 Flowchart of the compression moulding process

The last aspect needed for the compression moulding process is to determine the amount of material needed. The geometry of the cavity is a square with a side of 200mm and a single corner radius of 16mm, as can be seen in the upper right corner of the cavity in Figure 3-6. This corner radius reduces the surface area of the cavity only by 0,1% and it was decided not to take it into consideration. This means that slightly more material than needed will be placed in the cavity, helping to minimize the amount and size of voids. Equation 3-6 was used for the calculation and Table 3.3 lists the results.

$$m_{PL} = A_{PL} \times \rho_c \times t \quad (3-6)$$

Table 3.3 Weight of rLFT CF-PEEK needed for plates of varying thicknesses

A_{PL}	ρ_c	$m_{PL,2mm}$	$m_{PL,4mm}$	$m_{PL,6mm}$	$m_{PL,10mm}$	$m_{PL,20mm}$
400 [cm ²]	1,5763 [g/cm ³]	126,1 [g]	252,2 [g]	378,3 [g]	630,5 [g]	1261 [g]

3.3 Testing methodology

As stated in the introduction, one of the goals of this master thesis is to characterize the rLFT CF-PEEK material. This involves conducting mechanical tests, that subject samples to specific load cases, from which the basic strength and the ultimate strain of the material in that particular load case can be determined, as well as engineering constants like elastic modulus and Poisson's ratio. The load cases in question are tensile, compression, bending, shear and bearing pressure. An overview of all the strengths and engineering constants, that will be determined in the course of this master thesis, is given in Table 3.4. All tests needed to determine these parameters, with the exception of the compression shear test, which will be described later in this chapter, will be done according to standardized testing methods. The choice of test method is guided primarily by the testing jigs and fixtures available at LCC. Despite that, other test methods were considered and their advantages and disadvantages will be discussed below.

Table 3.4 Symbols used for strengths and engineering constants

Name	Symbol	Unit
Tensile strength	$\sigma_{m,t}$	<i>MPa</i>
Compressive strength	$\sigma_{m,c}$	<i>MPa</i>
Flexural strength	$\sigma_{m,f}$	<i>MPa</i>
In-plane shear strength	$\tau_{m,12}$	<i>MPa</i>
Apparent interlaminar shear strength	$\tau_{m,13} = \tau_{m,23}$	<i>MPa</i>
Plain-pin bearing strength	$\sigma_{m,p}$	<i>MPa</i>
Tensile modulus	E_t	<i>GPa</i>
Compressive modulus	E_c	<i>GPa</i>
Flexural modulus	E_f	<i>GPa</i>
In-plane shear modulus	G_{12}	<i>GPa</i>
Poisson's ratio in tension	$\nu_{12,t}$	-
Poisson's ratio in compression	$\nu_{12,c}$	-

3.3.1 Tensile testing

Tensile testing will be conducted according to the ISO 527 [23] standard, with the ASTM D3039 also being considered. As described in Chapter 3.2, the mould used produces 200x200mm plates, which means that the maximum length of a tensile sample is limited to 200mm. This is the main reason for not choosing the ASTM D3039, as the standard specifies a rectangular specimen geometry with a length of 250mm and width of 25mm for a random-discontinuous fibre orientation, which the rLFT material has. ISO 527-4 on the other hand recommends a Type 1 B specimen geometry for fibre reinforced thermoplastics with a minimum length of 150mm. The Type 1 B sample geometry is narrower in the middle, where the gauge length is located, as can be seen from Figure 3-11. This increases the axial stress σ_1 in that area due to the smaller cross section and also makes the sample more likely to fail there, rather than the grips. That is especially important when testing LFT since the discontinuous reinforcement creates local stress concentrations at the ends of the fibres and this increases the unpredictability of the failure location.

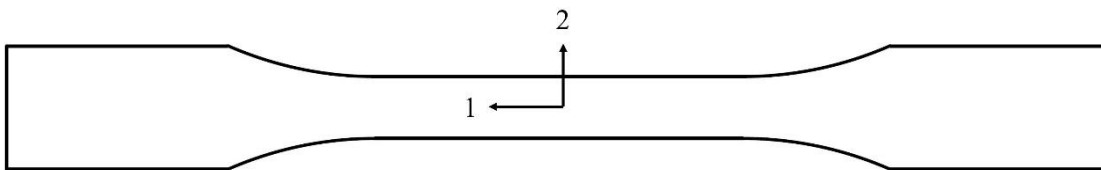


Figure 3-11 Type 1B sample according to ISO 527 with axes definition

The thickness of the samples was set to 4mm, since in Chapter 6.1 of the ISO 527 standard [23], a recommendation for the maximal thickness deviation for compression moulded materials of 2% is given. From previous experiments with the same mould, it is known, that the thickness deviation across a plate typically ranges between 0,08mm and 0,1mm, so a 4mm sample thickness is enough to ensure thickness variation within a sample of less than 2%. The overall length of the samples to be tested is 180mm.

The goal of the tensile testing is to determine the tensile strength $\sigma_{m,t}$, the elastic modulus in tension E_t , the Poisson's ratio in tension $\nu_{12,t}$. The testing of these parameters will be done on a UPM250 universal testing machine made by Hegewald & Peschke, which provides the force measurement thru a 250 kN load cell. The samples are held in the testing machine with a set of hydraulic grips. The pressure for those will be set to 120 bar, which equates to 105 kN clamping force. The measurement of the Poisson's ratio $\nu_{12,t}$

necessitates strain measurements in both the axial and transverse directions (1- and 2-directions). Using an optical method for these measurements compared to using strain gauges makes the sample preparation a lot easier and also allows measurement of large displacements. For these two reasons, an optical strain measurement method was used for the tensile testing. The LCC laboratory is equipped with two options for that - a digital imaging correlation (DIC) system and a video extensometer. The later uses markers in the form of black to white transitions (dark to bright transitions) and compares sequential images to determine how much the two markers moved relative to each other. The DIC will be explained in detail in Chapter 3.3.4.1, where it will be used to measure the in-plane shear properties of the rLFT material. A Pike F-210 video extensometer made by LIMESS GmbH will be used because of the significantly quicker setup and the better ease of use of the system, as well as the lack of post-processing of the raw data compared to the DIC method. In order to get measurements in both the 1- and 2-direction with the video extensometer, two sets of markers 90° to each other will be used. For the transverse direction (2-direction), the width of the sample itself will be used as w_0 and with a white light shining at the camera, the edges of the sample will form the two white to black transitions needed. The ISO 527-4 [23] prescribes a testing speed of 2 mm/min for qualification tests using Type 1B samples such as elastic modulus determination.

For the evaluation of the elastic modulus E_t and the Poisson's ratio $\nu_{12,t}$, the ISO 527 standard assumes a linear behaviour of the material between $\varepsilon'_{1,t} = 0,05\%$ and $\varepsilon''_{1,t} = 0,25\%$ and this part of the strain-stress curve is used to calculate the two engineering constants with Equation 3-8 and 3-9 respectively. Both of these equations use the secant method. This method is used in ISO 527 for the elastic modulus, but not for the Poisson's ratio. In order to keep the method consistent between tensile and compression testing, the secant method will be used for determining the Poisson's ratio and the modulus of elasticity in both load cases.

$$\sigma_t = F/(w \times t) \quad (3-7) \quad E_t = \frac{F'' - F'}{(\varepsilon''_{1,t} - \varepsilon'_{1,t}) \times w \times t} \quad (3-8)$$

$$\nu_{12,t} = -\frac{\varepsilon''_{2,t} - \varepsilon'_{2,t}}{\varepsilon''_{1,t} - \varepsilon'_{1,t}} \quad (3-9) \quad \varepsilon_{1,t} = \frac{L_0 - L}{L_0}; \quad \varepsilon_{2,t} = \frac{w_0 - w}{w_0}$$

3.3.2 Compression testing

The choice of standards for this type of testing was between the ISO 604 and the ASTM D6641M. The former requires the placement of 10x10x4mm samples for the strength testing and 50x10x4mm samples for the testing of the elastic modulus between two compression platens. The latter of the two methods uses combined loading compression (CLC) – a 140x13x4mm sample is fixed in a testing fixture, as shown in Figure 4-14. The load is then applied through both compressive stress on the open ends and shear stresses through the sides of the sample. This lowers the chance of the ends of the sample getting crushed, which reduces the risk of a sample needing to be discarded and not included in the results. Another consideration is the method for measuring the strains. The accessibility to the sample for cameras and lenses in both of these tests is severely limited, which necessitates the use of strain gauges. Due to the difficult and time-consuming process of applying them and the cost associated with the strain gauges themselves, the use of the CLC testing method is advisable, since it lowers the chance of a sample needing to be discarded. A further measure to lower the chance of a sample being damaged when clamped in the CLC test fixture or the sample slipping in said fixture is the application of tabs. These are made out of a 2mm thick fibreglass reinforced resin and are glued to the specimen with 3M™ Scotch-Weld™ DP490 two component epoxy glue in the grip areas of the sample. The tabs can be seen in Figure 3-12, as well as Figure 4-14, where they are the light-coloured parts between the CF-PEEK sample and the test fixture.

As mentioned previously, strain gauges will need to be used to measure the axial ε_{1c} and transverse ε_{2c} strains. The strain gauges chosen are the FCAB-5-11-1LJB-F type made by Tokyo Measuring Instruments Lab Co. Ltd. This particular strain gauge is a two-element type with the strain gauges arranged at 90° to each other. Both of the strain gauges have a gauge length of 5mm, resistance of 120Ω and a gauge factor of 2,08. Two of these double strain gauges will be used, one on each side of the sample in order to determine if the sample is bending. The strain gauges will be attached to the samples using cyanoacrylate glue. A QuantumX MX410B data acquisition module made by HMB GmbH will be connected to the UPM100 universal testing machine made by Hegewald & Peschke Meß- und Prüftechnik GmbH, on which the tests will be carried out. The test machine will capture and convert the signals from the strain gauges. A 100 kN load cell

will be used to measure the force. A testing speed of $1,3 \text{ mm}/\text{min}$ is prescribed in the standard [24].

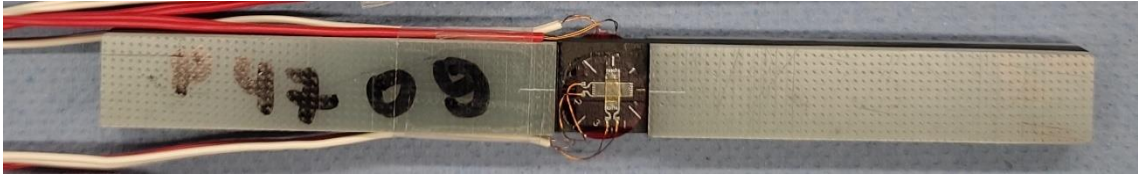


Figure 3-12 CLC sample with strain gauges applied to both sides

The calculations for the stress, modulus of elasticity and Poisson's ratio are identical to the ones used for the tensile testing with the only difference being the start and end points for the secant. The ASTM D6641 [24] standard prescribes $\varepsilon'_{1,c} = 0,1\%$ and $\varepsilon''_{1,c} = 0,3\%$. Equation 3-13 gives an opportunity to compare the measured value of the Poisson's ratio to the results from other experiments, as done by Selezneva and Lessard in [10].

$$\sigma_c = F/(w \times t) \quad (3-10) \quad E_c = \frac{F'' - F'}{(\varepsilon''_{1,c} - \varepsilon'_{1,c}) \times w \times t} \quad (3-11)$$

$$v_{12,c} = -\frac{\varepsilon''_{2,c} - \varepsilon'_{2,c}}{\varepsilon''_{1,c} - \varepsilon'_{1,c}} \quad (3-12) \quad v_{12} = \frac{E_{12}}{2 \times G_{12} - 1} \quad (3-13)$$

3.3.3 Flexural testing

This type of testing is the only one already conducted as a part of the term project. There, a 4-point flexural test was performed on 2mm thick samples. Here, the test will be used not only for the material characterization, but also to finish the test series from the term project, to examine the influence of the part thickness on the mechanical strength and to determine if the use of vacuum does translate into better mechanical performance.

The ISO14125 [25] gives two testing methods to choose from, when conducting flexural testing – a 3-point and a 4-point test. The difference between them is that the former has a single loading member, while the latter has two. Chapter 3 of the standard [25] states that the 4-point flexure benefits from lower compressive contact stresses due to the increased number of loading members and also has a constant bending moment between the loading members. The last point is especially important when testing LFT material, because the material tends to break between fibres or at their ends. When using 3-point flexure, if a break occurs anywhere but the centre line of the loading member, the stress

at which the failure occurred is unknown. This is because with 3-point flexure, the bending moment has a maximum at the centre line of the loading member and is lower anywhere else. Conversely, the 4-point flexure exhibits constant bending moment between its two loading members, which translates into constant bending stress. This means that as long as the failure takes place between the loading members, the bending stress is known and the exact position does not matter. This, coupled with the tendency of the LFT to break unpredictably, makes the 4-point flexure the better choice and is what will be used in this master's thesis.

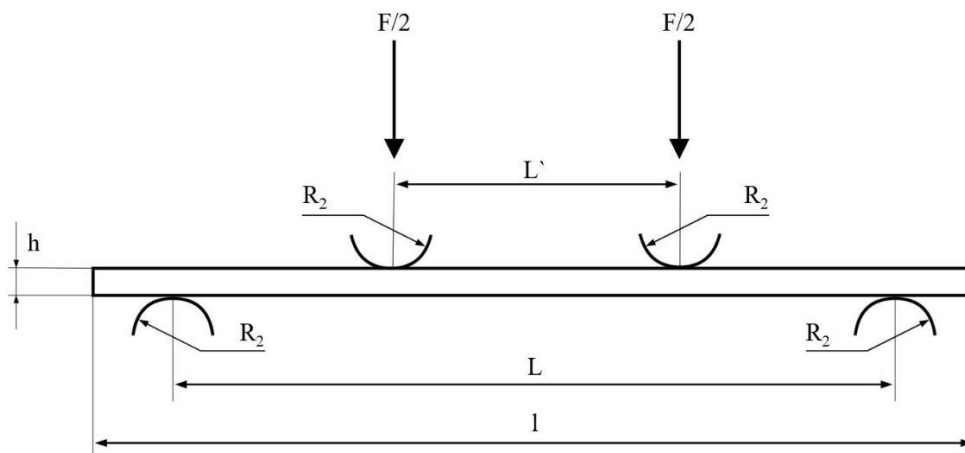


Figure 3-13 4-point flexure test setup

The test configuration for 4-point flexure is shown in Figure 3-13. The inner span L' is formed by the two loading members, which move vertically and apply the force to the sample. The outer span L consists of two supports, that do not move during the test. Both the loading members and the supports have a radius associated with them, which in the case of 4-point flexure is $R_2 = 2 \text{ mm}$ for samples thinner than 3mm and $R_2 = 5 \text{ mm}$ for specimen thicker than 3mm [25]. The sample is placed between the supports and the loading members and the loading members move down at a constant rate until the sample fails. The distances L and L' , as well as the length of the sample are all dependent on the thickness of the sample and the type of material tested. The LFT material fits Class II the best with other similar materials like bulk moulding compound (BMC) and fibre mats. For Class II material, Equations 3-14, 3-15 and 3-16 can be used to calculate L , L' and l . The information for the thicknesses to be tested in this master's thesis is summarized in Table 3.5. The width of all samples is 15mm, as per Table A2 from the ISO 14125 standard [25].

$$l = 20 \times h \quad (3-14) \quad L = 16,5 \times h \quad (3-15) \quad L' = 5,5 \times h \quad (3-16)$$

Table 3.5 Summary of parameters for flexural testing

<i>t</i>	2mm	4mm	6mm	10mm
<i>l</i>	40 mm	80 mm	120 mm	200 mm
<i>w</i>	15 mm	15 mm	15 mm	15 mm
<i>L</i>	33 mm	66 mm	99 mm	165 mm
<i>L'</i>	11 mm	22 mm	33 mm	55 mm
<i>R</i> ₂	2 mm	5 mm	5 mm	5 mm
<i>V</i>	1 mm/min	2 mm/min	5 mm/min	5 mm/min

The testing speed varies depending on the distance between the supports and should be adjusted, so that the strain rate is about 1% per minute [25]. Equation 3-19 was used to calculate the optimal speed for each thickness to be tested and the closest recommended speed from Table 1 in the standard [25] will be used for the tests. σ_f'' and σ_f' are the flexural stresses at $\varepsilon_f' = 0,05\%$ and $\varepsilon_f'' = 0,25\%$ respectively.

$$\sigma_f = \frac{F \times L}{w \times h^2} \quad (3-17) \quad E_f = 500 \times (\sigma_f'' - \sigma_f') \quad (3-18)$$

$$V = \frac{0,01 \times L^2}{4,7 \times h} \quad (3-19) \quad \varepsilon_f = \frac{4,7 \times s \times h}{L^2} \quad (3-20)$$

Testing will be carried out on a UPM100 universal testing machine equipped with a 10 kN load cell and made by Hegewald & Peschke Meß- und Prüftechnik GmbH. A 4-point flexure test rig with tiltable rollers for both the loading members and the supports will be used as well. The tilting feature allows the fixture to comply with samples that have twist in them or are otherwise not flat. The rollers eliminate the friction that can otherwise occur between fixed supports and the sample during the test. The strain measurement will be done using the same Pike F-210 video extensometer made by LIMESS GmbH, that will be used for the tensile testing as well.

3.3.4 Shear testing

Due to the anisotropic behaviour of the LFT material, two separate tests with shear loading need to be performed – one with the shear acting in the 12-plane and one in the 13-/23-plane.

3.3.4.1 In-plane shear strength

For this test, three methods were considered – V-notched beam method in ASTM D5379, V-notched rail shear method in ASTM D7078 and the shear testing using a shear frame in DIN EN ISO 20337. Out of the three methods, only the last one induces pure shear loading in the specimen and it is the first choice of testing method, however LCC is not equipped with such test jig. It also has to be noted, that the samples needed for the testing with a shear frame are quite large at 165x165x4mm [26] and significantly bigger than the samples needed for the other two tests. On the other end of the spectrum is the sample for the V-notched beam test, which has an overall width of 19mm and only 11,4mm in the notched section. This means that only one to two 12x12mm chips will be present in the notched area of sample and these are insufficient to create a quasi-isotropic behaviour. The V-notched rail shear sample from ASTM D7078, with its 30,6mm wide notched section, strikes the best balance between the sample being too small or too big, out of the three testing methods taken into consideration here. For this reason, the V-notched rail shear is the test of choice for this master's thesis. The specimen for this test is 76mm wide and 56mm tall with two 90° notches, which reduce the area on which the shear force acts to 30,6mm times the specimen thickness, 4mm in this case. Figure 3-14 shows the sample shape and the grip areas, which are the rectangles on the left and right side enclosed by the dashed lines. The tensile load is applied in the 1-direction, which causes a shear stress in the 12-plane. This stress is strongest in the section between the two V-notches because the cross-sectional area there is the smallest.

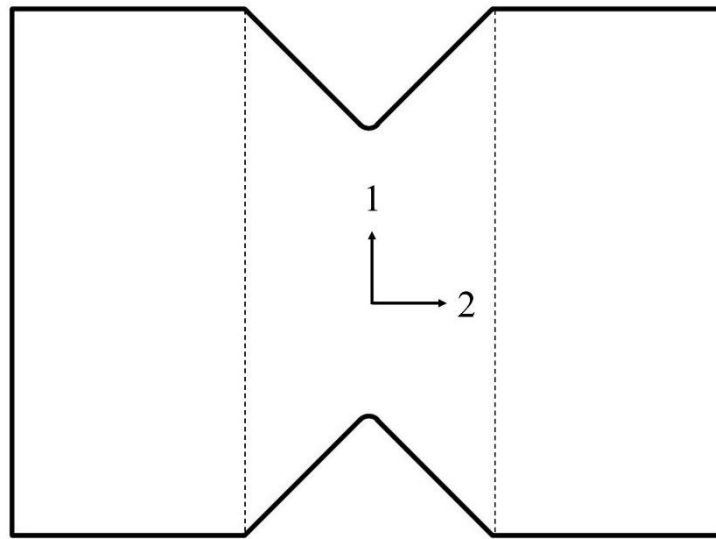


Figure 3-14 Sample for V-notched rail shear test with axes definition

The sample, as mounted in the test fixture, is shown in Figure 4-17. The bolts that clamp the specimen are tightened to 55Nm using a torque wrench as per the standard [27]. On the left side of the figure, the speckle pattern for the strain measurement is visible, as well as in Figure 4-18. That pattern consists of a white background with fine black dots on top of it and is required for the functioning of the digital image correlation technique that was used to capture displacements and strains. The DIC works by comparing the positions of the black dots from one frame to the next and by tracking these, a displacement field is generated, from which a strain field and other parameters of interest can be calculated. By using a system called Aramis, that utilises two ARAMIS 4M cameras angled relative to one another, the ARAMIS Professional 2020 software is capable of tracing the black points in the speckle pattern in three dimensions. This allows not only to gather the engineering shear strain γ_{12} needed for the calculation of the shear modulus G_{12} , but also to detect any bending in the sample, both while mounting it in the test jig and during the test. One benefit of the DIC system used here is its ability to capture the complete displacement field, on the part of the sample that has the speckle pattern on it. In contrast, strain gauges measure only in one point and only in the direction they are designed for and placed at. The DIC also allows the calculation of new parameters of interest at a later date, as long as the image data is saved. Equations 3-21 and 3-22 will be used to calculate the parameters needed from the test. A test speed of 2 mm/min , as well as a strain range from $\gamma'_{12} = 0,15\%$ to $\gamma''_{12} = 0,55\%$ for the determination of the shear modulus G_{12} will be used during testing, as recommended in the ASTM D7078 standard [27].

$$\tau_{12} = \frac{F}{t \times w_{notch}} \quad (3-21)$$

$$G_{12} = \frac{\tau_{12}'' - \tau_{12}'}{\gamma_{12}'' - \gamma_{12}'} \quad (3-22)$$

3.3.4.2 Interlaminar shear strength

The testing of the interlaminar shear strength will be done using the short-beam method from the ISO 14130 standard. The ASTM D2344 also uses the short-beam principle and has very similar setup and test procedure. The short-beam test is a type of 3-point flexure test, where the distance between the supports is relatively small, causing large interlaminar shear stresses to develop. The sample size of 20x10x2mm, compared to the normal 3-point flexure sample of 40x15x2mm, illustrates the significant reduction in the outer span of the test setup. There is no strain measurement for this test, the only result is the apparent interlaminar shear strength $\tau_{m,13}$, which due to the quasi-isotropy of the LFT material in the 12-plane is the same for any plane perpendicular to the 12-plane, meaning $\tau_{m,13} = \tau_{m,23}$. Equation 3-23 is used to calculate $\tau_{m,13}$ with w being the width and h being the thickness of the sample. The testing will be done on a UPM100 universal testing machine made by Hegewald & Peschke Meß- und Prüftechnik GmbH and a purpose-built test fixture. The testing speed given in the ISO 14130 [28] for the test is 1 mm/min.

$$\tau_{13} = \frac{3}{4} \frac{F}{w \times h} \quad (3-23)$$

3.3.5 Compression Shear testing

While planning the tests for this master's thesis, an opportunity came up to use a testing method developed by the Polymer Competence Center Leoben GmbH (PCCL). The test was primarily developed for glued joints, but can be used to apply shear loads to composite materials. Figure 3-15 shows a diagram of the test setup. The sample is placed between the fixed support on the bottom and the loading member on the top, while the two movable supports on the side keep the sample from rotating during the test. The left movable support and the loading member move together along the 1-axis and in doing so, the loading member applies a compressive load F_c to the sample.

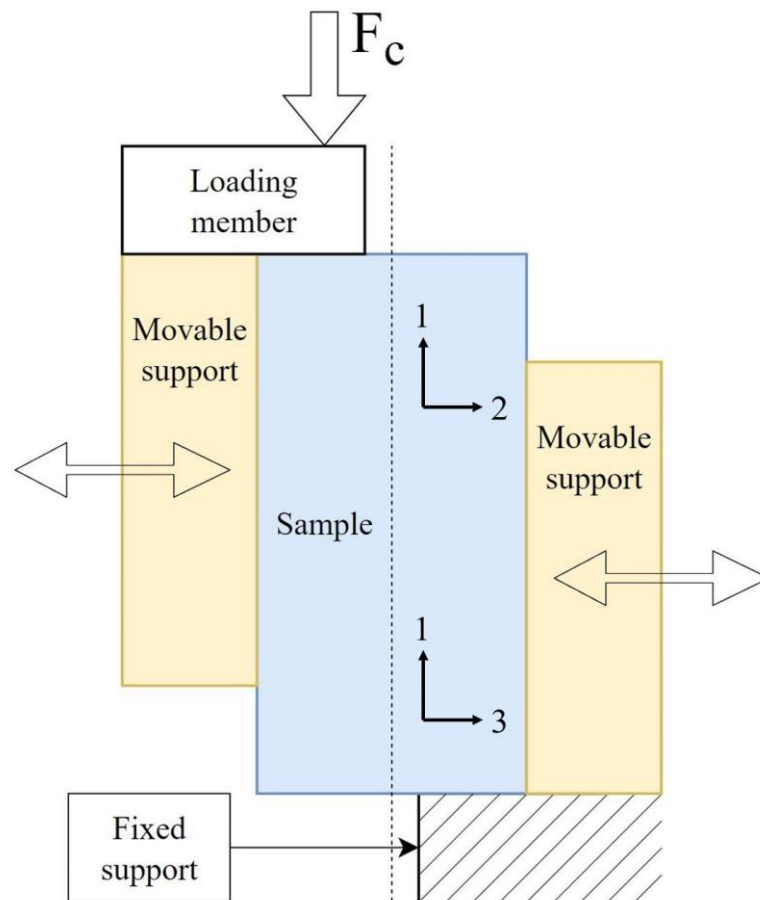


Figure 3-15 Schematic diagram of the compression shear test

The advantages of this method are small sample size and easy test setup. The sample size used here is 20x10x4mm, but smaller and or thicker samples also are able to fit in the test jig provided by PCCL. The specimen is not clamped in the test jig, rather placed on the fixed support and held in place by the movable supports. This makes changing the sample in the test jig very quick, which contrasts to experiments such as the V-notched rail shear and the combined loading compression, where clamping a sample takes a substantial amount of time. One drawback of the test setup is the relatively small contact area between the sample and the fixed support or the loading member respectively. This has the potential to cause crushing of the ends, when the force F_c exceeds the compressive strength of the material tested. Another consideration when choosing whether to use this testing method is the fact, that it is internal to the PCCL and is not an internationally recognized and standardized test procedure. Further consideration when testing LFT material with this method is the relatively small size sample used. Except for the smallest chip size of 6mm, both the 12mm and 18mm chips are larger than the width of the sample and comparable to its height. This means, that the sample has at best a few and at worst a

single chip spanning one of its dimensions. Consequently, there are not enough randomly oriented fibres to assume quasi-isotropy of the material, which in turn makes the mechanical properties of the sample strongly dependent on the local fibre orientation and length.

The compression shear test will be used to obtain values for both in-plane and interlaminar shear strengths. This will be done by orienting either the 12- or the 13-plane of the samples respectively, so that it matches the plane depicted in Figure 3-15. The test will be carried out on a UPM100 universal testing machine made by Hegewald & Peschke Meß- und Prüftechnik GmbH, using a 10 kN load cell and the test jig provided by PCCL. Test speed was chosen to be $1,5 \text{ mm/min}$ for all of the testing. Displacement measurement will not be conducted. The strengths will be calculated by dividing the maximal force recorded by the cross-sectional area of the sample in the action plane.

3.3.6 Plain-pin bearing test

As discussed previously, the compression moulding process allows complex geometries to be manufactured in a cost and time efficient way. Such complex parts are very likely to be joined to other components using bolted joints, therefore it is important to include a test that simulates such loading in the material characterization. In order to keep the testing simple and not specific to threaded fasteners, a plain-pin bearing test will be conducted instead. Three standards, which involve plain-pin bearing testing, were identified – the ISO 12815, ASTM D5961 and the ASTM D953. The first two tests are specifically for CFRPs, while the latter is not. Because test jigs for none of these tests were available, one needed to be procured or made. Due to the simplicity of the jig for the ISO 12815, that test was chosen to be used here and a test jig to be made in house at LCC. The testing setup is shown in Figure 3-16. The test is a tensile one with a sample placed in one of the machine's grips, while a test jig is placed in the other.

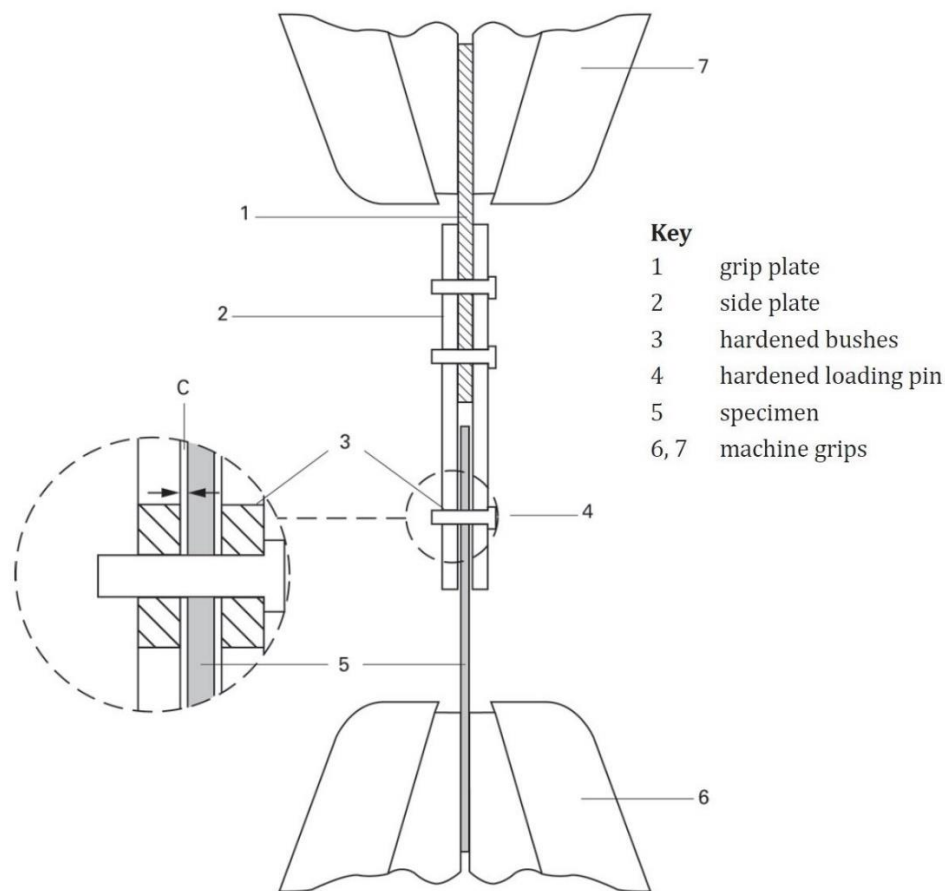


Figure 3-16 Test setup for plain-pin bearing strength according to ISO 12815 [29]

The test jig contains the loading pin, which goes through a hole in the sample and in this manner only the hole is loaded during the tensile test. The test jig required for the test was not available at the LCC laboratory due to plain-pin bearing strength tests not being commonplace when testing composite materials. For this purpose, the jig in Figure 3-17 was designed and manufactured. As suggested in the ISO 12815 standard, two drill bushings from hardened metal were used for the spot where the loading pin goes through the side plates. The three plates were machined from mild steel and standard cylindrical pins were used for both the loading pin and the two load transmitting pins in the top of the jig. The middle plate was made 6mm thick, so that a 4mm thick sample has enough clearance between it and the side plates, as is required in the standard [29].

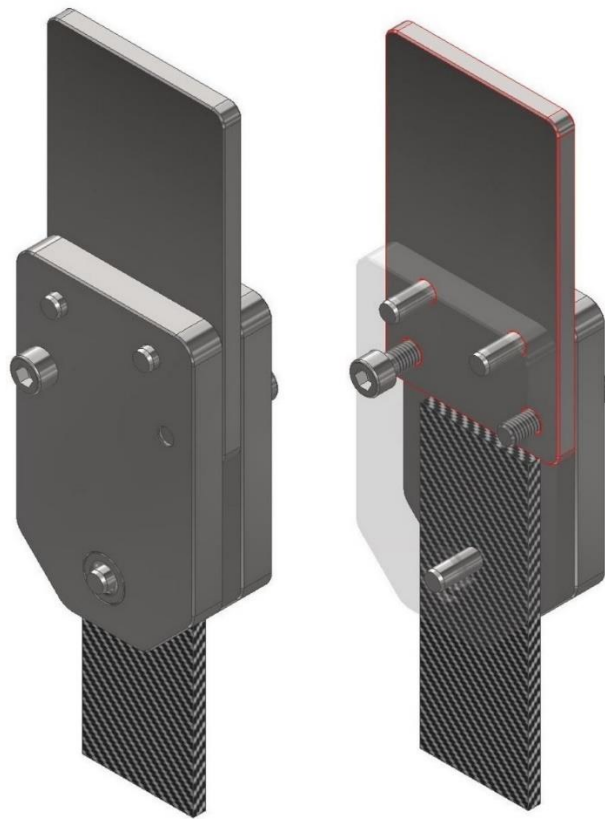


Figure 3-17 Test jig for ISO 12815 plain pin bearing strength test

The test itself will be conducted similarly to the tensile test on a UPM250 using a 250 kN load cell and hydraulic grips. The hydraulic pressure used in this case will be 80 bar, which will clamp the sample with a force of 70 kN. Testing speed will be 1 *mm/min*, as per the standard [29]. The sample will follow the geometry given in the standard of 4mm thickness, 36mm wide and a hole 6mm in diameter, located in the middle of the sample width wise and 36mm from the top edge. The overall length of the sample will be 100mm. The samples to be tested will not only be made from rLFT material, but a special laminate will be manufactured and tested also, in order to gain comparative values for continuously reinforced CF-PEEK material. The ISO 12815 standard suggests a pseudo-isotropic stack-up for the laminate, while Schürmann [7] recommends a stack-up consisting of 50% 0° layers, 10% 90° layers and 40% ±45° layers for maximum strength in this load case. The latter layer configuration with a stack-up of [(0°/0°/+45°/0°/-45°/90°/+45°/0°/-45°/0°/+45°/0°/-45°/0°)s, 90°] will be used here. Equation 3-24 is used to calculate the plain-pin bearing strength $\sigma_{m,p}$.

$$\sigma_p = \frac{F}{d \times h} \quad (3-24)$$

3.4 Design of Experiment

As part of the term project, that precedes this master's thesis, the compression moulding process was analysed and the relevant process parameters were determined. As described in Chapter 3.2, these are the compaction pressure p_{PL} , the pressing temperature T_{press} , the time spent at pressing temperature t_{press} and the chip size. Due to the inability to effectively control t_{press} , it was decided to exclude it from the parameter study. The remaining three parameters were used as variables in a test series, the goal of which is to determine the best set of parameters, that result in parts with the highest mechanical strength possible. In order to reduce the effort it will take to conduct that test series, a design of experiment (DoE) methodology was used. It encompasses the planning, design and analysis of an experiment and aims to allow for test series to be carried out robustly and with minimal effort [30]. In order to achieve that, the DoE method uses statistical modelling to represent the relationships between the process parameters, also called factors, and the mechanical strength, which is the output of the test series. In the term project and in this master's thesis, the statistical modelling was handled by a specialized software called MODDE12, that is made by Sartorius Stedim Data Analytics AB. Within that software, response surface modelling (RSM) was used, as it is most suitable to the optimization of parameter space task at hand [30]. RSM is capable of using up to quadratic polynomials to estimate the effect the factors have on the output. The D-Optimal type of response surface modelling was used, as it resulted in the highest power, when using two factors with five levels each, one factor with three levels and twenty-one experiments in total. The first two factors are the temperature and pressure and the third factor is chip size. The levels are as follows: pressing temperature T_{press} with 380°C, 395°C, 410°C, 425°C and 440°C, the compaction pressure p_{PL} with 10 bar, 35 bar, 60 bar, 85 bar and 110 bar, and chip size with 6mm, 12mm and 18mm. The resulting test matrix for the 21 experiments can be seen in Table 3.6. The evaluation of the mechanical strength will be done using flexural testing, the choosing of which is described in the term project [18].

Table 3.6 Test plan for the DoE test series

Exp. №	T [°C]	p [bar]	CS [mm]
N1	380	10	6
N2	425	10	6
N3	440	10	6
N4	380	35	6
N5	440	85	6
N6	380	110	6
N7	395	110	6
N8	440	110	6
N9	380	10	18
N10	440	10	18
N11	425	35	18
N12	395	85	18
N13	380	110	18
N14	440	110	18
N15	395	10	12
N16	440	35	12
N17	380	85	12
N18	425	110	12
N19	410	60	12
N20	410	60	12
N21	410	60	12

4 Results

In this chapter the knowledge and results gathered as part of this master's thesis will be presented and compared, when possible, with the state of the art.

4.1 rLFT CF-PEEK after compression moulding

Compression moulded parts from long fibre reinforced CF-PEEK exhibit a structure similar to continuously reinforced laminates in that both have distinct layers, as can be seen from Figure 4-1 and Figure 4-5. The first figure shows a cross section of a quasi-isotropic laminate, that was made in the same mould and at the same process parameters as all of the other rLFT plates. Its layers are flat and oriented parallel to the 12-plane of the plate (12-plane illustrated in Figure 3-2), as can be expected from a fibre reinforced laminate. In contrast, the layers of the rLFT material shown in Figure 4-5 are not planar and also generally not parallel to the 12-plane of the plate. This waviness of the layers is detrimental to most of the strengths, due to the fibre axes not being completely aligned with the load plane. On the other hand, the undulations of the layers make the area, in which an interlaminar shear stress acts larger, hence increasing the loading force needed to cause an interlaminar failure. Examples of that will be shown in Chapter 4.7.2, where the results of the compression shear test will be presented. These layer undulations are caused by uneven distribution of chips, which as the practice showed, is hard to detect while filling the mould cavity. The potential for such uneven distributions becomes more pronounced with thicker cross sections because of the increased volume the uncompacted chips occupy. Further, a large chip size increases the likelihood of uneven distributions because the tendency of the chips to interlock and clump together gets higher. Figure 4-2 thru Figure 4-5 exemplify this phenomenon. The undulations could be reduced with more advanced strategies for placing the CF-PEEK chips in the mould cavity. Such strategies were not examined as part of this master's thesis.

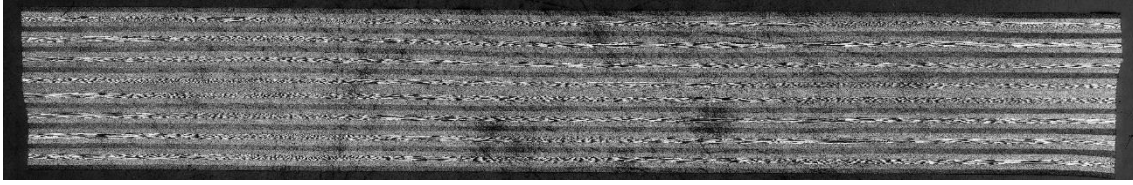


Figure 4-1 Cross section of 4,48mm thick quasi-isotropic compression moulded laminate with a $(0^\circ/-45^\circ/90^\circ/+45^\circ)_8s$ stacking sequence at 5x magnification



Figure 4-2 Cross section of 2mm thick rLFT CF-PEEK plate at 5x magnification

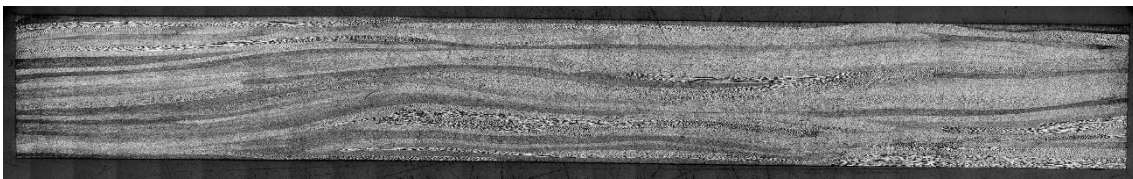


Figure 4-3 Cross section of 4mm thick rLFT CF-PEEK plate at 5x magnification

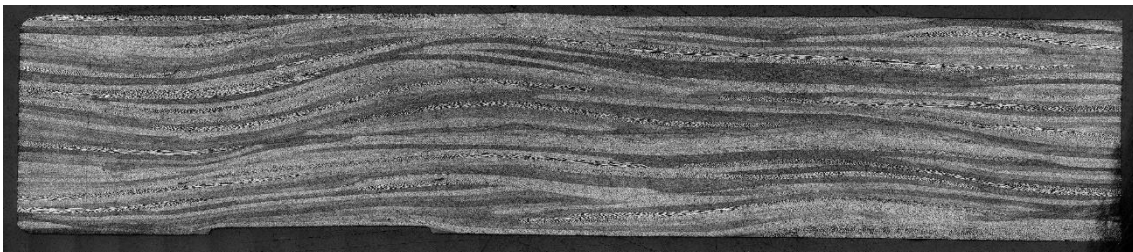


Figure 4-4 Cross section of 6mm thick rLFT CF-PEEK plate at 5x magnification



Figure 4-5 Cross section of 10mm thick rLFT CF-PEEK plate 5x magnification

A problem, that was observed with a significant number of the 2mm thick plates pressed, is warping. This is not unique to this master's thesis, as Selezneva and Lessard in [10] observed a similar problem. There, the authors found a significant amount of warping in their 2,5mm thick plates, while their 6mm plates experienced little to no warpage. This is consistent with the observations made in this master's thesis – the 4mm, 6mm and 10mm

plates exhibited no visible warping, while most of the 2mm plates had an obvious warping. The most likely reason for the occurrence of warping is the varying fibre orientation between different areas and layers of the plate and the fact that a UD layer of CF-PEEK exhibits significantly different coefficients of thermal expansion (CTE) along its 1-axis compared to the 2- and 3-axis, as shown by Melo and Radford in [31]. Selezneva and Lessard [10] give similar reasoning for the warping - heterogeneous chip distribution and different CTEs. The warping of the different plates was not quantified in this master's thesis.

4.2 Optimal Parameters

As can be seen from the test plan in Chapter 3.4, the test plan includes 21 experiments. The manufacturing of the plates, as well as the flexural testing was split between the term project and this master's thesis with 9 experiments carried out during the former and the remaining 12 during the latter.

The results of the flexural testing for the DoE test series can be seen in Figure 4-6 and Figure 4-7. These values are an average from 5 to 7 samples, depending on how many of the 7 samples taken from each plate failed in an acceptable way. The highest average flexural strength of 646,8 MPa is achieved by N10, the lowest is 377,9 MPa by N7, the highest average flexural modulus of 40,26 GPa resulted from testing N11, while N9 with 28,3 GPa had the smallest average flexural modulus of all the plates tested. The flexural strength does show an increase with the longer 12mm and 18mm fibres, when compared to 6mm chips. The same comparison of the flexural modulus does show the same general trend, albeit not as clearly. Both of these effects are in line with the expected effect from increasing the fibre length. Experiments N19, N20 and N21 are replicates and are used by the statistical model to form the centre of the parameter space. Comparing them also allows to evaluate how much the mechanical properties can vary between specimen pressed at the same parameters. The difference between plates N20 and N19 is 11,4% for the flexural strength and 11,9% for the flexural modulus.

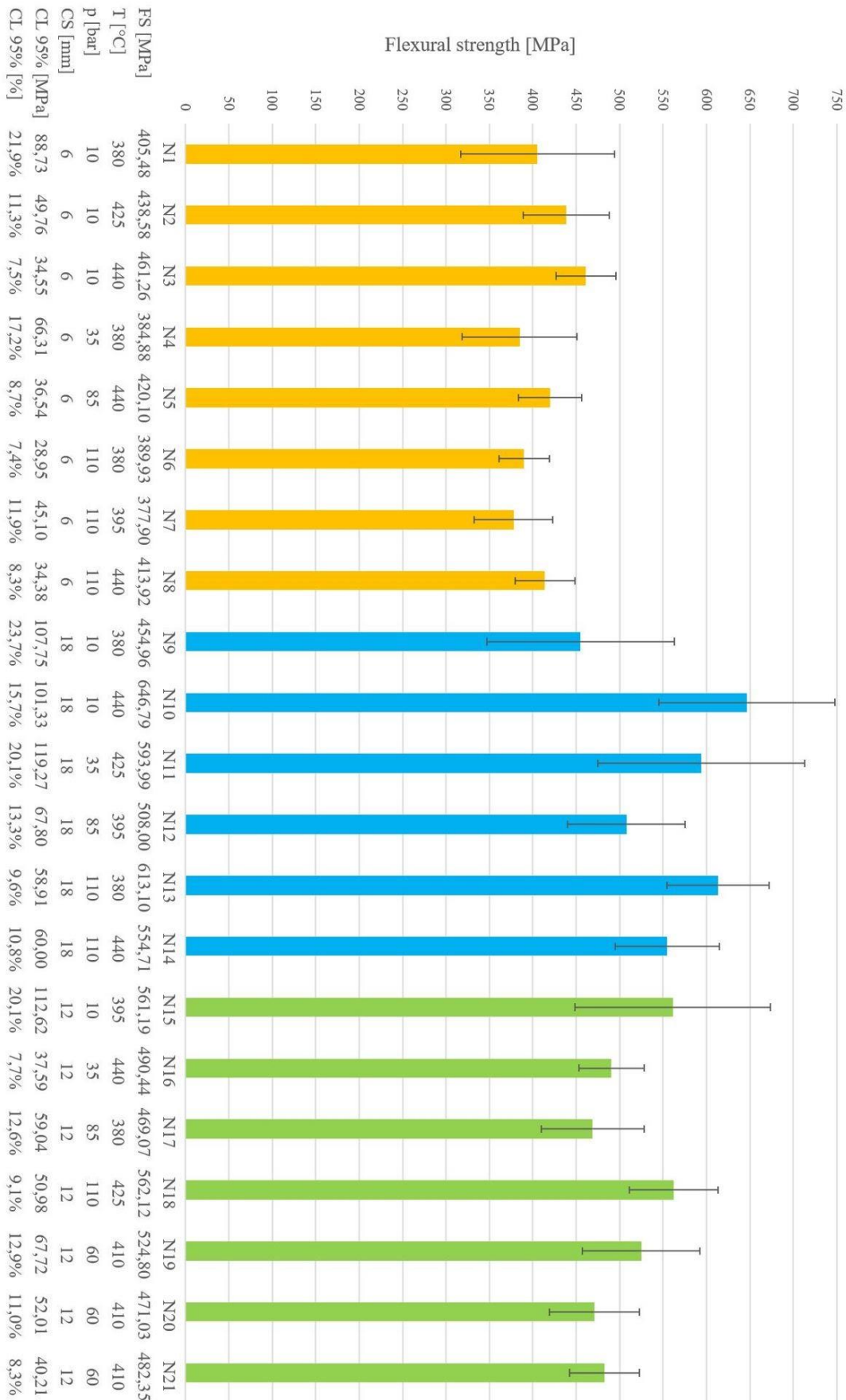


Figure 4-6 Summary of flexural strengths for the DoE statistical modelling

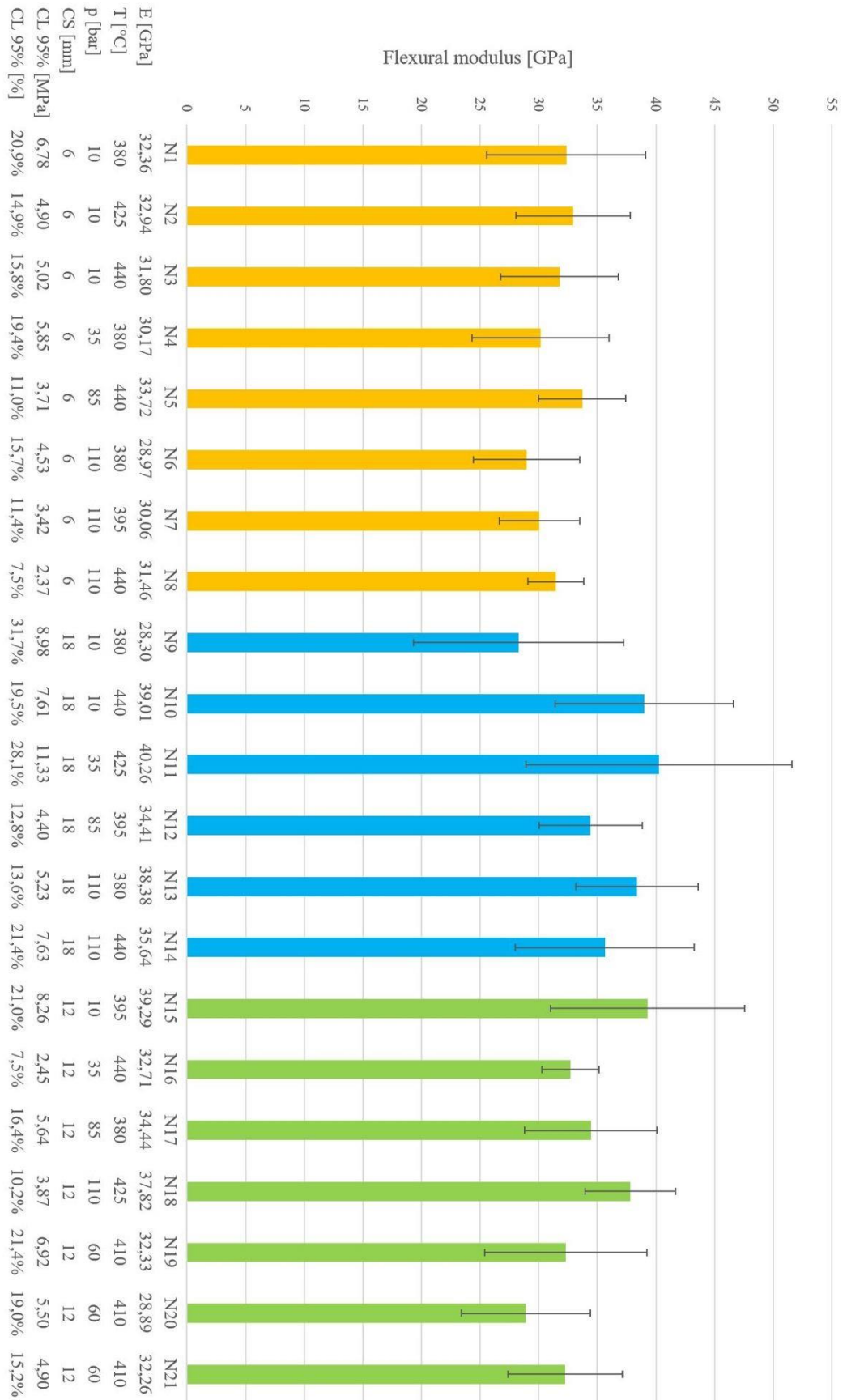


Figure 4-7 Summary of flexural moduli for the DoE statistical modelling

The values obtained for the flexural strength and modulus, together with the 95% confidence intervals, which are used here to evaluate variability, are then plugged into the statistical model created with MODDE. The first step in the evaluation is to determine if the statistical model fits the data well using the coefficients of the model, their interactions and the parameters R², Q², Reproducibility and Model validity. R² is a measure of how well the model fits the data, Q² quantifies how well the model expects new data. Reproducibility of one means that if the study is conducted once again with the same input parameters, the result will be the same. Model validity shows how correct the model is. Partial least squares regression (PLS) was found to fit the data better than multiple linear regression, so the former was used. After the parameters and interactions, that are not statistically relevant, are removed from the model, its fit can be judged based on the R², Q², Reproducibility and Model validity parameters. In order to have a representative statistical model, R² needs to be over 0,5, Q² should be larger than zero and have a difference compared to R² of less than 0,3, the model validity should be bigger than 0,25 and the reproducibility should be as high as possible [30]. The models for all the model outputs include all process parameters at the start, as well as their interactions and MODDE builds an independent model for each output. In order to improve the R², Q², Reproducibility and Model Validity, MODDE analyses which model terms are not statistically significant for each individual model and if removing them improves the Q² value of the respective model, then they are removed. The remaining model terms for each of the outputs can be seen in the coefficient plot in Figure 7-1. The summary of fit after the elimination of the statistically not significant model terms can be seen in Figure 4-8. When the criteria for R² to be higher than 0,5 is applied to the summary of fit in Figure 4-8, it becomes apparent, that the statistical model is not able to fit the data for the flexural modulus well because the R² value of 0,344 is under the threshold. For this reason, the flexural modulus and its variability will be excluded from the analysis.

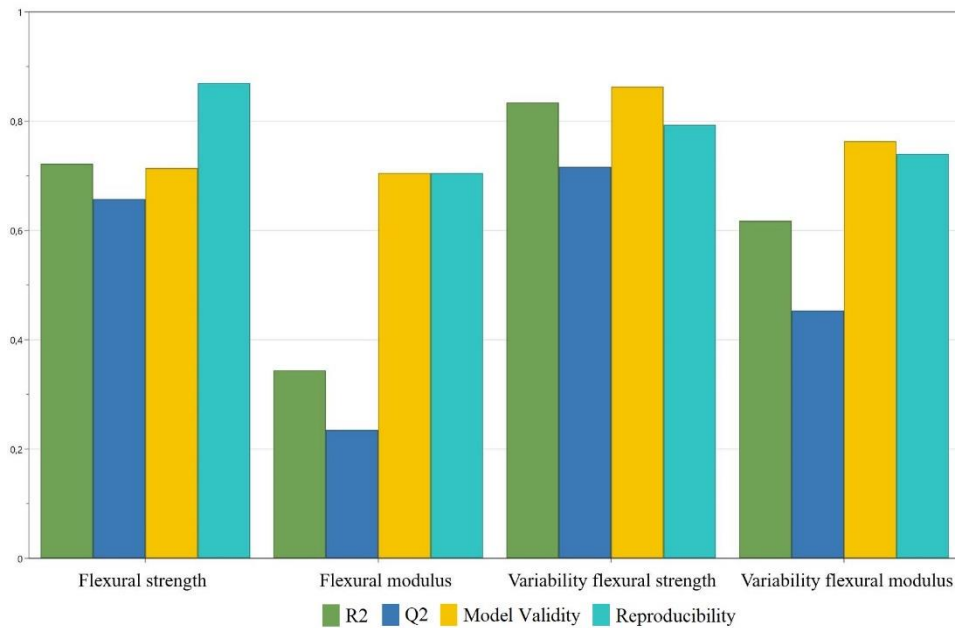


Figure 4-8 Summary of fit for the statistical model from MODDE

The coefficient plot in Figure 7-1 shows something interesting – the process parameter pressure has been determined to not be statistically significant for both the flexural strength and flexural modulus and has been removed from their statistical models. This is consistent with the fact, that once the mould is closed, the majority of the force applied by the hydraulic press is not turned into further compaction pressure at the plate, but is simply putting more compressive load on the mould itself. This means that the pressure is not a process parameter and as long as the condition of a complete mould closure is satisfied, no continuous monitoring or precise control of the pressure applied by the hydraulic press is needed. In this case, the hydraulic pump can operate discontinuously by only turning on after the pressure falls under a certain threshold, which is still greater than the minimum pressure needed to close the mould. This discontinuous operation is more energy efficient and can contribute to lowering the cost of the recycling process. LeBlanc et al. observe in [19] a similar phenomenon, where pressures above 10 bar do not lead to better filling of the rib geometry the authors are testing, regardless of the strand size they use. On the other hand, both the variability of the strength and the modulus show a dependency from the pressure. This may hint at the fact that while full mould closure is enough to achieve maximal strength, the speed with which the closed state is reached might have an effect on the compaction and flow of the CF-PEEK material and in turn the variability.

The result for the optimal parameters given by the statistical model was the N10 experiment that produced the highest flexural strength: 440°C, 110 bar and 18mm chips. The 95% confidence levels of the flexural strength and modulus of N10 are 15,7% and 19,5% respectively. Figure 4-9 and Figure 4-10 show what the statistical model predicts for the flexural strength and flexural strength variability for different combinations of process parameters. While a high mechanical strength of the rLFT CF-PEEK material is the goal of this study, the variability also plays an important role when it comes to practical applications. Further, the quasi-isotropic material properties of rLFT only manifest, when a parts in-plane dimensions are substantially larger than the fibre length. Increasing chip size also provides a larger area, where interlaminar cracks can propagate unhindered. For these reasons, 12mm chips are going to be used in this material characterization. Minimizing the variability is also the reason why the highest pressure of 110 bar will be used, as the response plot in Figure 4-10 suggests. Further, processing of PEEK at a temperature under 400°C and in combination with non-oxidizing atmosphere was found by Day et al. in [21] to be beneficial for minimizing degradation of the PEEK matrix. Lower processing temperatures also have the benefit of being more energy efficient. For these two reasons, the processing temperature of 395°C will be used.

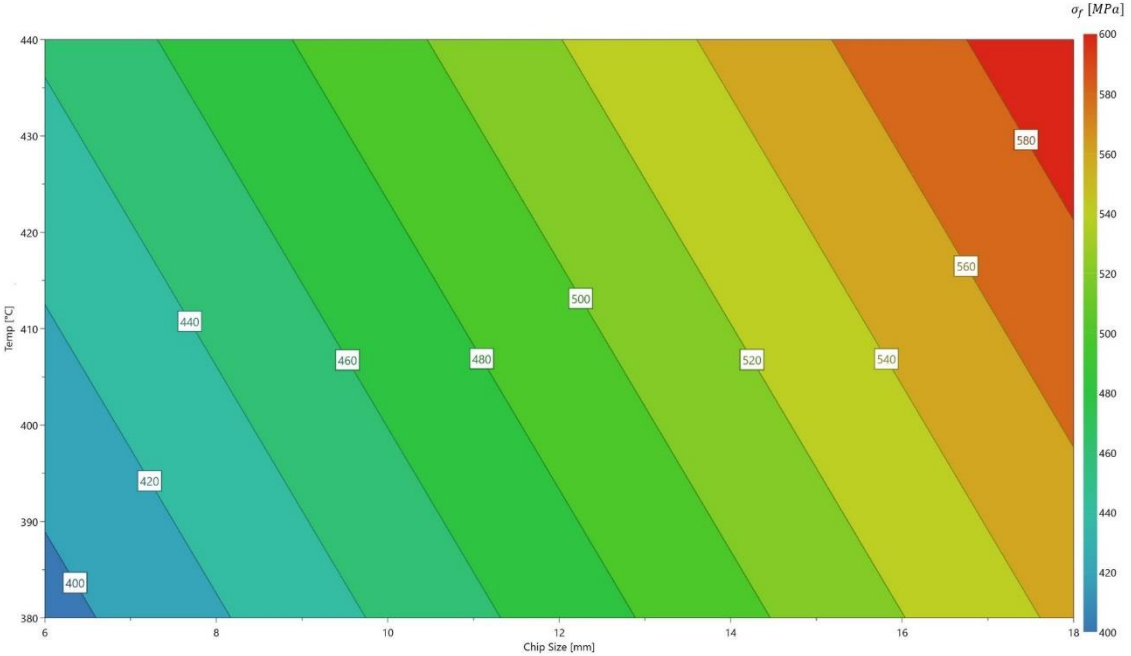


Figure 4-9 Response contour plot of the flexural strength from MODDE

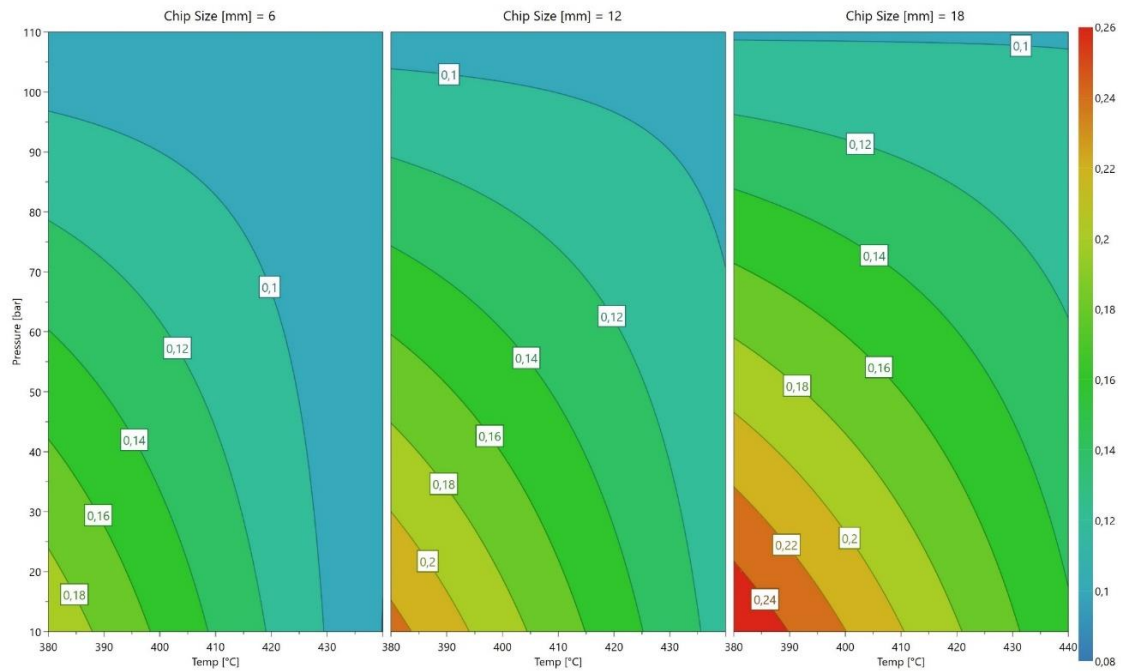


Figure 4-10 Response contour plot of flexural strength variability as a fraction of flexural strength, from MODDE

The process parameters of 395°C, 110 bar and 12x12mm chips will be used for all of the plates made for the material characterization. The only exception will be the laminate specially made for comparing to the rLFT, when measuring the pin bearing strength. That laminate will be processed at the same temperature and pressure, but made from continuously reinforced CF-PEEK.

A 2mm plate with the optimal parameters had to be made for the study of the influence cross section thickness has on the strength and elastic modulus of rLFT CF-PEEK material. Since the study was done using the same flexural testing as the DoE study, the results from that plate provide an opportunity to check how well the statistical model can predict the strength and its variability. According to the model, a 2mm plate processed at 395°C and 110 bar and made out of 12x12mm chips should have a flexural strength of 482 MPa and a 95% confidence level of that flexural strength of less than 10%. The measured average strength is 476,3 MPa with a 95% confidence level of 8,3%. This means, that the model was able to predict both the strength and the confidence interval of the optimal set of parameters very closely. This however, is the only set of parameters for which the accuracy of prediction was checked and further testing would be needed to verify that aspect of the statistical model.

4.3 Influence of cross-sectional thickness

The examination of the variation in mechanical strength with the thickness of a part is done in this master's thesis by analysing the results from flexural tests on 2mm, 4mm, 6mm and 10mm samples. The plates, from which the samples originate, are manufactured using the optimal parameters from Chapter 4.2. The 4-point flexural test according to the ISO 14125 standard, that is used here, is summarized in Chapter 3.3.3. 17, 16, 10 and 9 samples were tested from the 2mm, 4mm, 6mm and 10mm thicknesses respectively with 12, 13, 5 and 7 samples breaking in an acceptable way, inside the inner span.

Figure 4-11 shows the average flexural strength of different thicknesses of samples tested. The error bars represent the 95% confidence interval. The flexural strength shows a trend of decrease with increasing sample thickness. The difference in strength between the 2 or 4mm and 10mm samples is statistically significant. Also, with the exception of the 6mm samples, the variability of the results decreases with thicker cross-sections. The 95% confidence level of the flexural strengths are 8,3%, 5,72% and 4,34% for the 2mm, 4mm and 10mm thick samples respectively. The average strength and the confidence interval for the 6mm samples are calculated from only 5 samples. Due to that low number of samples, the confidence interval is wider, which in turn makes coming to an unequivocal conclusion not possible.

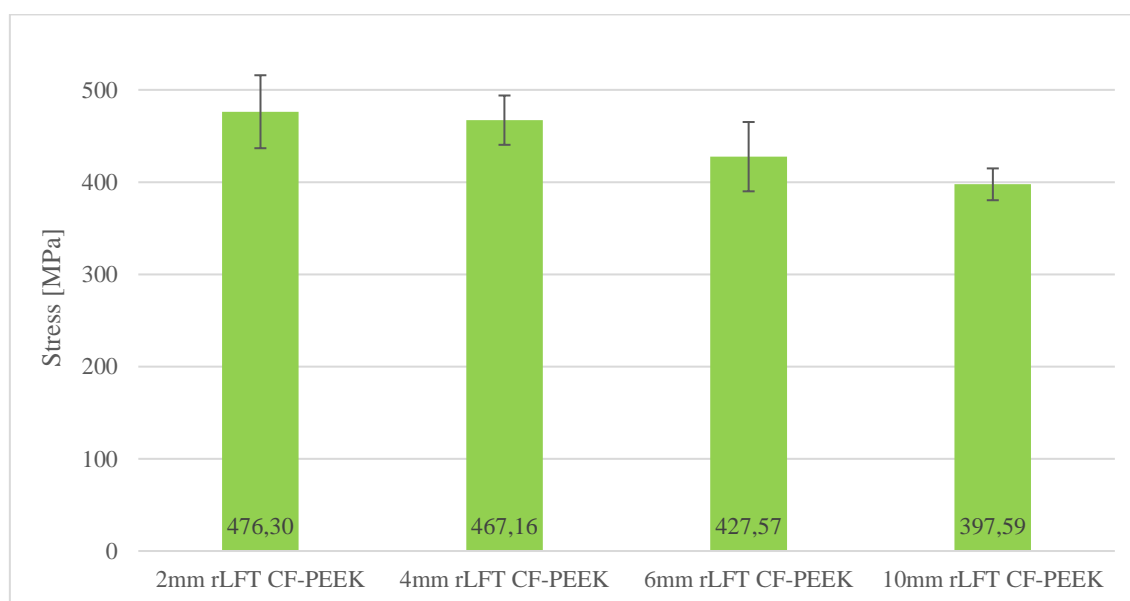


Figure 4-11 Flexural strength of 2mm, 4mm 6mm and 10mm thick rLFT CF-PEEK

The lower flexural strength of the thicker samples can be explained by the proportional relationship between the inner span L' (the distance between the loading members, where

the flexural stress is the highest) and the sample thickness h , which is $L' = 5,5 \times h$. This increase in the size of the inner span, combined with the fact that the chip size and sample width remain the same for all specimen, means that the number of chips in a single layer, that is inside the inner span, also increases proportionally to the thickness. A greater quantity of discrete CF-PEEK pieces in the rLFT material equates to more fibre ends at which stress concentrations arise, from which a crack can start to form. For the same reason, the increased thickness of a sample, which is achieved by adding more layers of chips, directly contributes to lower flexural strength. The increased number of stress concentrations makes it more likely for thick samples to fail at a lower stress level than a thinner one, at least when purely flexural loads are concerned.

Figure 4-12 shows the flexural modulus of the samples tested for this comparison. As in Figure 4-11, the error bars here represent the 95% confidence level interval. The three thickest plates exhibit similar flexural modulus and the differences between them are not statistically significant. Further the flexural modulus of the tested 2mm plate is the lowest ever tested for 12x12mm chips, as can be seen when comparing with experiments N15 thru N21 from Figure 4-7. This can be explained by an unfavourable orientation of the chips in the test plate used for the 2mm flexural test. The variability of the average flexural modulus behaves like the one for the average flexural strength and decreases with thicker cross-sections, with the exception of the 6mm samples for reasons explained previously.

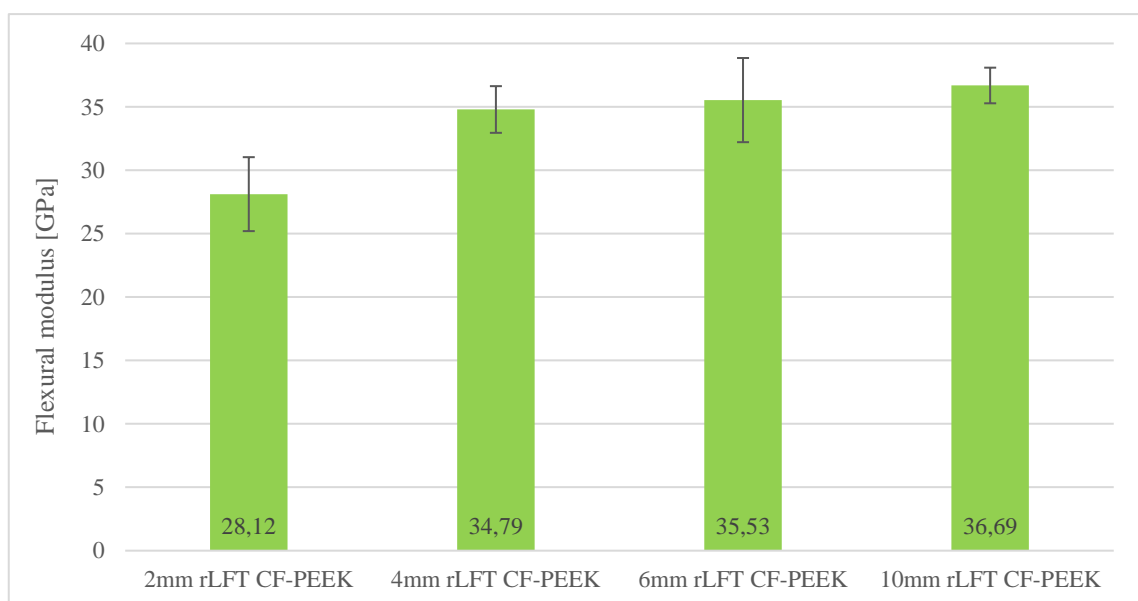


Figure 4-12 Flexural modulus of 2mm, 4mm 6mm and 10mm thick rLFT CF-PEEK

The microscopy of the 4 plates, examples of which can be seen in Chapter 4.1, did not reveal voids in any of the places on the plates, that have been sampled. This means that

voids are unlikely to be the cause of the decrease in flexural strength observed here. It also means that, at least when processing cross-sections of up to 10mm under vacuum, the quality of the compression moulding process is not influenced by how thick the part is. This implies that the reduction in flexural strength is caused by the testing methodology of the ISO 14125 flexural test as explained earlier in this chapter. It should be noted, that the geometry tested here, a plate, is a simple one and the statement above regarding the compression moulding process may not apply to complex geometric shapes.

4.4 Tensile testing

The experiment done to determine the tensile properties of the rLFT CF-PEEK material ran into a problem with the measurement of the transverse strain. Due to the use of the sample edges as gauge length in the transverse direction and the poor quality of said edges after the waterjet process used to cut the samples, the video extensometer had difficulties in measuring the small displacements in the transverse direction. This manifested as high amount of noise in the transverse strain signal coming from the video extensometer. As a consequence, no Poisson's ratio in tension $\nu_{12,t}$ was produced by the test. This problem would not have been present, if the DIC system was used for the strain measurement. In the loading direction, no problem with noise presented itself due to using of suitable markers. In order to increase the friction in the grip area and prevent slipping, the ends of the samples were media blasted to both remove the releasing agent and create a rough texture of the surface.

Out of the 18 samples tested, 7 samples failed outside the gauge length of the Type 1B sample. The results from the other 11 were averaged to a tensile strength of 263,46 MPa with a 95% confidence interval of 32,05 MPa (12,16%) and an elastic modulus of 38,51 GPa with a 95% confidence interval of 3,08 GPa (8%). All eleven samples failed due to individual chips sliding relative to each other. Figure 4-13 shows the tensile samples before testing, the white stickers are the markers for the video extensometer and denote the gauge length.



Figure 4-13 Type 1B tensile samples for testing according to ISO 527

4.5 Compression testing

This combined loading compression (CLC) test was conducted according to ASTM D6641 and also used the test fixture described in the standard. It is depicted in Figure 4-14. The 140x13x4mm CF-PEEK samples, which are 8mm thick in the grip areas, were mounted in the test jig using the procedure described in the standard and the clamping bolts were tightened to 3 Nm. This torque was sufficient to ensure the ends of all twelve samples tested did not get crushed. Samples were dried at 60°C for 6 hours prior to testing.

As described in Chapter 3.3.2, the strains in both the axial and transverse directions (1- and 2-axis) were measured on the front, as well as the back of all the samples. The application of strain gauges on both sides of the samples enables the monitoring of any bending or buckling that might occur. Bending of the sample manifests itself in the signal from the strain gauges as difference in the strain of two strain gauges on opposite sides of the sample, that measure along the same axis. ASTM D6641 provides a metric in the form of the percent bending with which to gauge the amount of bending that occurs. Equation 4-1 and Equation 4-2 show how the percentage bending around the 1- and 2-axis is calculated.

$$B_2 = \frac{\varepsilon_{1,L} - \varepsilon_{1,R}}{\varepsilon_{1,L} + \varepsilon_{1,R}} \times 100 \quad (4-1)$$

$$B_1 = \frac{\varepsilon_{2,L} - \varepsilon_{2,R}}{\varepsilon_{2,L} + \varepsilon_{2,R}} \times 100 \quad (4-2)$$



Figure 4-14 Combined loading compression fixture with a sample installed, after testing, strain gauge wires already removed

Figure 4-15 shows an example of a CLC sample and the strains that were measured during the test. The solid lines are the two strains along the 1-direction, while the dotted lines are the strains along the 2- or transverse axis. The left and right side of the sample are as seen in Figure 4-14. As can be seen when comparing the strains in the respective directions to each other, both the axial and transverse directions show differences in the strain values between the left and right side, which means that the sample experiences bending around both axes. All ten of the samples, that failed in an acceptable way, show bending around the 2-axis, while all but two samples also show bending around the 1-axis. Due to the diverging of the two strain signals from the start and not suddenly after an arbitrary point during the test, it can be concluded that the occurring phenomenon is not buckling. Further, the bending direction was not the same for all samples tested with three bending to the left and seven bending to the right. This excludes systematic error in the test setup as a possible reason for the bending. This only leaves the structure of the rLFT material as an explanation for the bending, either the left and right sides of the samples have different stiffnesses or the chips at the surface do. Although unlikely, it is possible that

the difference in strains is caused only by the orientation of the chips on the surface where the strain gauges are glued and the divergences of the strains are not representative of the whole sample. Due to the difficulty of determining which one is the true cause, an examination of it was not conducted as a part of this master's thesis.

For the evaluation of the elastic modulus and the Poisson's ratio, an average of the left and right side for each of the strains was used. The averaging should remove the strains caused by bending from the overall strain. The compressive strength was calculated as an average from ten samples to 348,8 MPa with a 95% confidence interval of 20,8 MPa or 5,96%. Both the elastic modulus E_c and the Poisson's ratio $\nu_{12,c}$ were calculated using the secant method using the averaged strains $\varepsilon'_{1,c} = 0,1\%$ and $\varepsilon''_{1,c} = 0,3\%$. The elastic modulus has an average value of 39,47 GPa with a 95% confidence interval of 3,87 GPa or 9,81%. The calculated values for the Poisson's ratio of the individual samples are split into two groups with three samples in the 0,372 to 0,407 range and six samples in the 0,192 to 0,254 range. Wang et al. examine in [32], among other things, the Poisson's ratio of PEEK polymer and Fig. 8 of the paper gives a value of around 0,403 for PEEK at room temperature (300K) and low pressures. This means that the first group of three samples either has fibres predominantly oriented roughly along the 2-axis, where the properties of the PEEK dominate the mechanical properties of the whole composite, or the chips on the surface of the sample do. For this reason, the second group of Poisson's ratios is considered correct and its values will be used as the result. The Poisson's ratio, calculated from 6 samples, is 0,2249 with a 95% confidence interval of 0,0216 or 9,59%. This result is in line with the comparative values for the Poisson's ratio calculated using Equation 3-13, the shear modulus G_{12} and the elastic modulus in tension E_t or compression E_c . The former comes to 0,1971 and the latter to 0,2271. The average Poisson's ratio from all 9 samples is 0,2785 with a 95% confidence interval of 0,0635 or 22,8%.

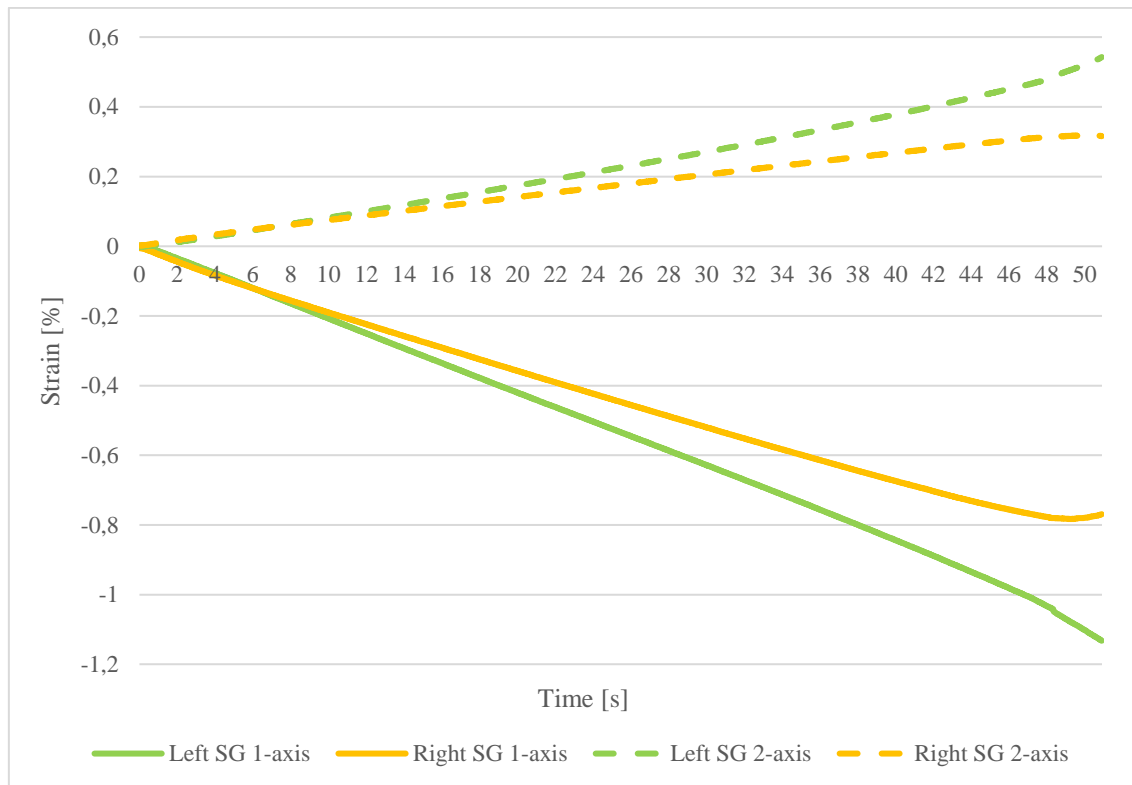


Figure 4-15 Axial and transvers strains from CLC sample number P4806 with double sided application of strain gauges (SG)

Figure 4-15 shows sample P4805 after the testing was conducted. It has been cut in half, polished and put under a microscope at 5x magnification. This sample is representative of the failure mode, that occurred with all CLC samples tested. The sample shown has expanded in width due to the interlaminar cracks that have formed and the gliding of different layers of chips relative to each other. Most notably, no fibre kinking is visible, because most of the fibres are oriented roughly perpendicular to the sample surface, which means their axes are not pointing in the load direction. These fibres manifest in Figure 4-16 as white dots, while the white lines and ovals are fibres, that are roughly parallel with the surface of the sample. Hence why it can be concluded, that the failure of sample P4805 is due to the meso-structure of the rLFT material. As can be seen especially on the left side of the sample, long interlaminar cracks can form, that reach significant distances away from where the fracture originates. Two of the twelve samples tested were excluded because such interlaminar cracks reached into the grip area.

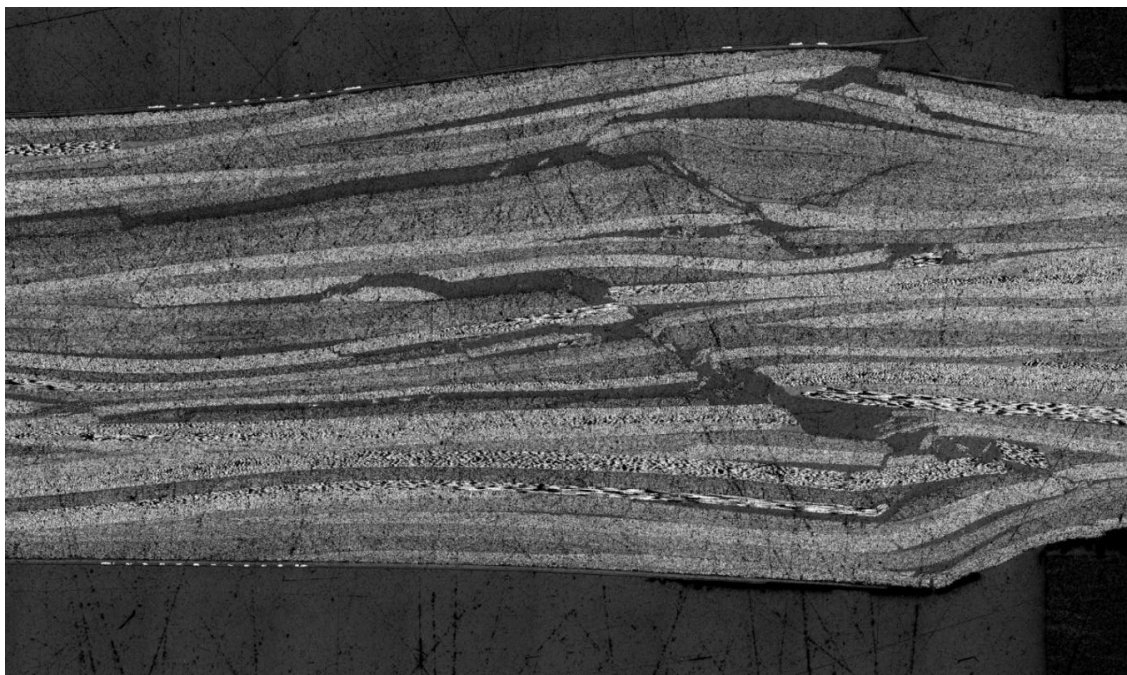


Figure 4-16 Cross section of CLC sample number P4805 after testing at 5x magnification

4.6 Flexural testing

The examination of the flexural strength was done using the recommended sample size for a Class II material of 80x15x4mm. For the evaluation of the relationship between part thickness and mechanical properties, 2mm, 6mm and 10mm thick samples were also tested, the results for which are discussed in Chapter 4.3. 16 samples were tested and 13 failed in an acceptable way – inside the inners span, between the loading members. The average strength from these 13 samples is 467,16 MPa with a 95% confidence level of 26,74 MPa or 5,72%. The average flexural modulus achieved by the samples is 34,79 GPa with a 95% confidence level of 1,84 GPa or 5,29%. Ten of the samples failed due to tensile fracture including interlaminar shear, two failed due to compressive fracture including interlaminar shear and one sample exhibited both of the failure modes above.

4.7 Shear testing

For the evaluation of the shear strengths, three different tests were performed – V-notched rail shear test, short beam test and a compression shear test.

4.7.1 In-plane shear

The V-notched rail shear test from ASTM D7078 was used to examine the in-plane shear properties of the rLFT CF-PEEK material. As can be seen from Figure 3-2, the 12-plane is the one in which the fibres should be oriented. The testing was conducted using 9 samples from two plates, both of which made at the optimal parameters from Chapter 4.2. The samples were clamped in the test jig shown in Figure 4-17 and the clamping bolts were tightened to the 55 Nm recommended in the ASTM D7078 standard. The DIC measurement was conducted using the ARAMIS system described in Chapter 3.3.4.1. A 3mm wide strip in the middle of the sample, as shown in Figure 4-18, was used to measure the shear strain using an area averaging method. Out of the 9 samples, 8 failed with a crack originating in the smallest cross section, which is the correct failure mode. These 8 samples have an average in-plane shear strength $\tau_{m,12}$ of 235,3 MPa with a 95% confidence level of 11,28 MPa or 4,79%. The in-plane shear modulus G_{12} is 16,08 GPa with a 95% confidence level of 1,18 GPa or 7,35%.

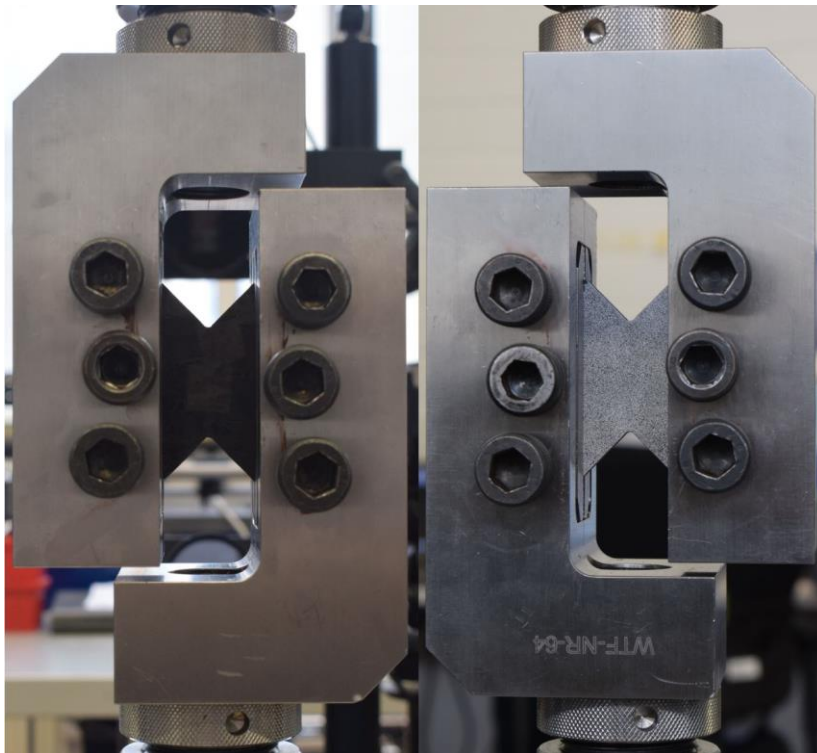


Figure 4-17 In-plane shear sample mounted in the V-notched rail shear test jig

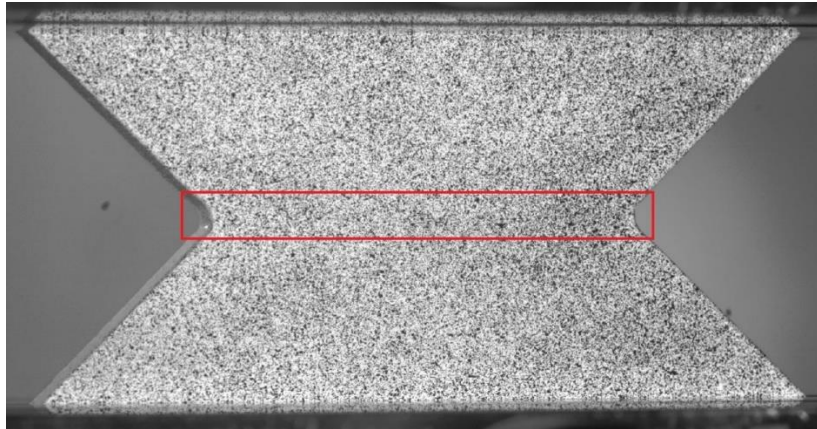


Figure 4-18 V-notched rail shear sample with the area used for measuring shear strain indicated by a red rectangle

An attempt was made to determine the in-plane shear using the compression shear test as well. In that case, a 20x10x4mm sample was oriented with its 12-plane as shown in Figure 3-15. The test was unsuccessful due to crushing of the sample ends.

4.7.2 Interlaminar shear testing

The short beam test according to ISO 14130 was conducted using 16 samples with the recommended geometry of 20x10x2mm. The samples were taken from a 2mm thick plate pressed using the optimal parameters from Chapter 4.2. None of the samples tested failed due to pure interlaminar shear, but rather due to a tensile break of the bottom layer, plastic deformation or a combination of both. Two samples did exhibit interlaminar crack running from the edge of the sample inwards, but in both cases the samples ultimately failed through tensile break. These results indicate that the rLFT CF-PEEK material with 12mm long fibre reinforcement possesses a comparatively high ILS strength, and failures of the material due to delamination are not going to be as common as in unidirectionally reinforced CF-PEEK. Figure 4-19 shows three samples from the test: the top most failed due to tensile break, but did exhibit an interlaminar break as well, the middle one deformed plastically with some delamination on the left side of the loading member and the bottom one experienced a tensile break of the bottom layer.



Figure 4-19 Failure modes of ISO 14130 samples: a) partial interlaminar crack from left side towards middle, tensile break; b) plastic deformation and partial layer separation; c) pure tensile break of the bottom most layer

As shown in Chapter 3.3.5, the compression shear testing method can be used for ILS testing as well, so 16 samples, 20x10x4mm in size, were tested. Out of them, only 5 failed due to interlaminar shear stresses, while all others exhibited compression damage on the sides, where the force was being applied. Just like with the ILS testing according to ISO 14130, the primary failure mode is not the one the test should induce. The five samples, that did fail due to ILS stress, did so at an average apparent ILS stress of 32,49 MPa with a 95% confidence level of 7,39 MPa or 22,75%. This value should be thought of as a lower limit of the ILS strength, because the 5 samples, from which the averaged value is comprised, are the weakest ones and not representative of the whole test group. Miao et al. reports in his publication [33] average ILS strength values for UD CF-PEEK of between 45,79 MPa and 49,95 MPa. So, it can be assumed, that the actual ILS strength of the rLFT CF-PEEK material is somewhere between 32,49 MPa and 49,95 MPa.

One possibility to reduce the chance of crushing the ends and help induce an interlaminar failure with the compression shear test is to reduce the area of the action plane. This can be achieved by for example halving the length of the sample used here and using a 10x10x4mm one, which should also halve the compressive force F_c . The problem with this approach when testing rLFT material is that the sample becomes smaller than the chips and the reinforcement effectively turns into continuous one on the scale of the sample. This makes the sample not representative of a rLFT material. At this point the sample is also too small to effectively capture the typical undulations in a rLFT part or in

this case plate. As can be seen from Figure 4-20, the failure surface is not planar, which as discussed in Chapter 4.1 increases the area of the action plane and the apparent ILS strength as well.

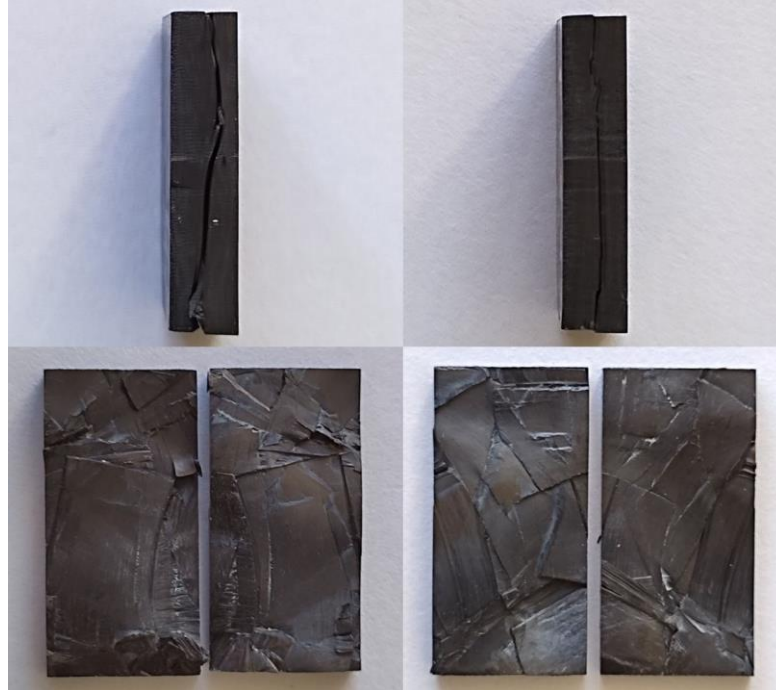


Figure 4-20 Two samples for the determination of ILS strength using compression shear testing, after testing

4.8 Plain-pin bearing strength testing

For this test, 9 samples from the rLFT CF-PEEK and 10 samples from the CF-PEEK laminate, that is optimized for bearing strength, were planned to be tested. All plates were pressed at the optimal parameters from Chapter 4.2. Due to manufacturing difficulties with the samples, only the rLFT samples were tested. Seven out of these nine samples were averaged to result in a plain pin bearing strength of 475,4 MPa with a 95% confidence interval of 17,64 MPa or 3,7% of the mean value. All of the samples tested failed because of bearing stresses and none through direct tension or shear-out. The failure due to bearing loading is shown in Figure 4-21. Two of the nine samples were excluded, because one was loaded multiple times while setting up the test and one was an outlier, that failed at only 77,6% of the bearing strength.

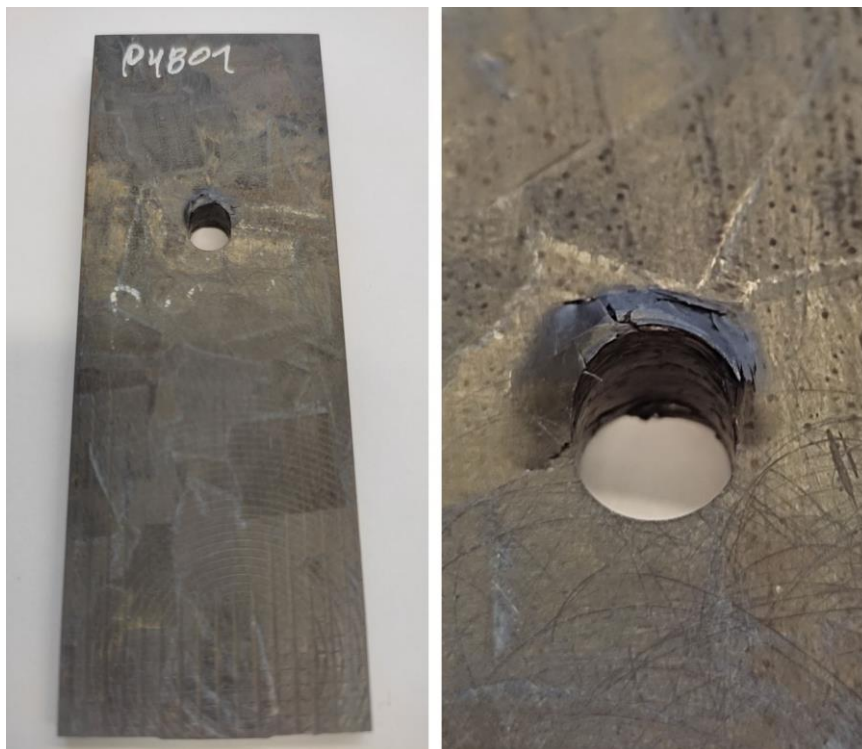


Figure 4-21 Plain pin bearing strength sample P4801 after testing



Figure 4-22 Plain pin bearing strength sample P4809 tested beyond its yield point: Left – complete sample; Right – close up of tested area

The last sample from this test series was loaded beyond its bearing strength in order to determine if other failure modes occur, when large displacements of the pin through the material are present. Figure 4-22 shows the sample after the test. The total displacement of the 6mm pin through the sample reached 13mm, at which point the test was terminated,

because the gap between the sample and test jig had become filled with plastically deformed material. Even after this amount of damage, the rLFT CF-PEEK sample did not fail through direct tension or shear-out.

Figure 4-23 shows a diagram of the forces while testing samples P4806 and P4809. The first sample shows a force curve typical for a bearing failure – the force rises until the bearing strength is reached, after which a plastic deformation takes place and the force decreases. After a while though, the bearing surface starts to increase as the plastically deformed material becomes able to carry some load and the force increases again. When that point is reached, the test is stopped, as suggested in the ISO 12815 standard [29]. The load on sample P4809 was released after reaching that point and then again loaded and the force from that is the green line in Figure 4-23. The increases in strength can be explained by the increase in bearing surface, while the reductions in force by the material plastically deforming and not being able to carry any more load.

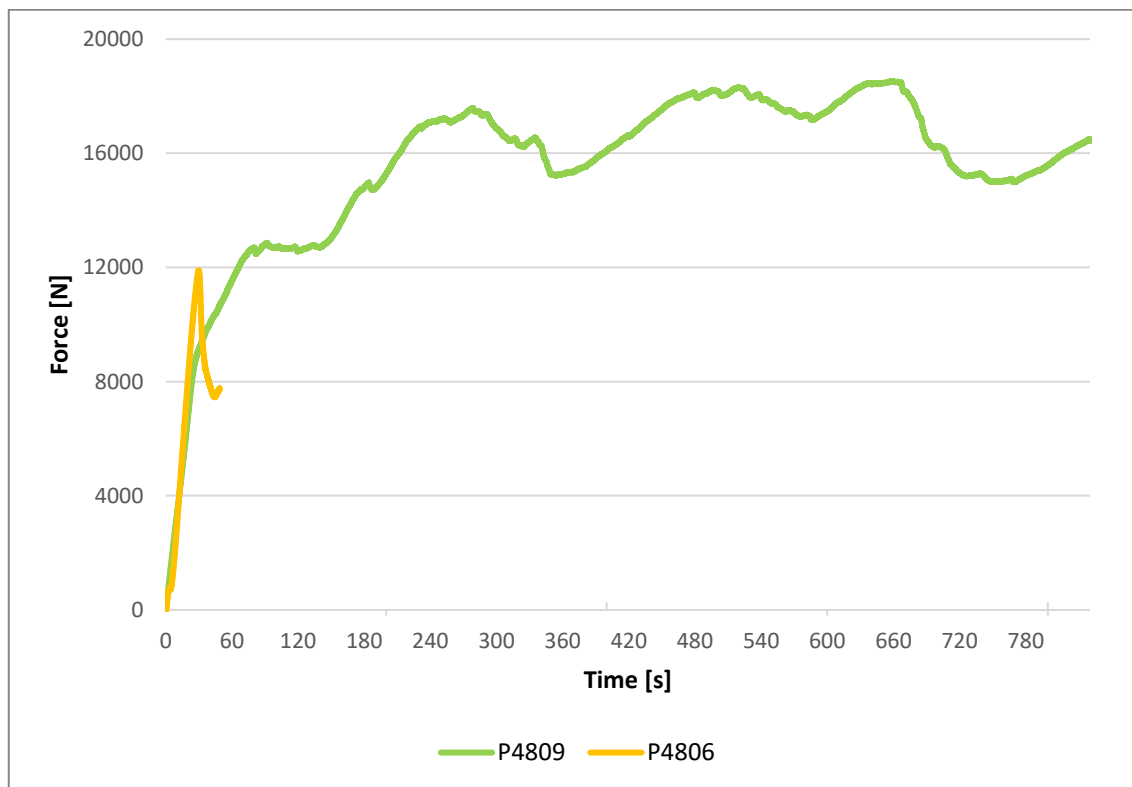


Figure 4-23 Force diagram of samples P4806 and P4809 during plain-pin bearing testing

4.9 Influence of vacuum during processing

Processing under vacuum has been an integral part of the experiments so far. Due to the need for air tightness of press or mould the vacuum brings and the vacuum pump it requires, it is important to know if the additional effort equates to the expected improvement in mechanical properties. For this reason, an additional experiment using the optimal parameters from Chapter 4.2 but in the presence of air was conducted. From the resulting 4mm plate, 14 flexural samples like the ones in Chapter 4.6 were cut and tested. The resulting flexural strength from 12 samples of 437,1 MPa with a 95% confidence level of 27,62 MPa or 6,32% is lower than the 467,2 MPa of the 4mm plate processed under vacuum by 6,89%. The flexural modulus is 35,13 GPa with a 95% confidence level of 2,19 GPa of 6,24%. In comparison, the flexural modulus of the plate pressed with vacuum is nearly identical at 34,79 GPa. Both of these differences are not statistically significant as the 95% confidence intervals of the respective values overlap each other. Also, the plate-to-plate variation of the process is comparable to the differences observed here, so there is no discernible trend as well. Further testing using average values from 5 plates of each type should be able to provide robust average values, that can be conclusively compared. Due to time constraints, this was not performed as part of this master's thesis.

4.10 Overview of the results

Table 4.1 gives a summary of the measured strengths and engineering constants for 4mm thick samples made from 12x12mm chips at optimal parameters during the material characterization in this master's thesis.

Selezneva and Lessard comment in their summary of mechanical properties in [10], that the compressive strength is higher than the tensile strength, the tensile and shear strengths are similar and so are the elastic moduli in compression and tension. The same observations can be made here, meaning that the qualitative behaviour of the results in both the publication and this master's thesis are the same.

As stated previously, the compression moulding process excels at creating complex geometries, which by their nature create stress states with multiple different stresses

acting. The rLFT CF-PEEK material is suited to such loads because of the well-rounded set of strengths it has, with the bending and the compression ones being of particular note.

Table 4.1 Overview of strengths and engineering constants for 4mm samples of 12x12mm rLFT pressed at 395°C and 110 bar

Name	Symbol	Value	Unit
Tensile strength	$\sigma_{m,t}$	263,46	<i>MPa</i>
Compressive strength	$\sigma_{m,c}$	348,80	<i>MPa</i>
Flexural strength	$\sigma_{m,f}$	467,16	<i>MPa</i>
In-plane shear strength	$\tau_{m,12}$	235,30	<i>MPa</i>
Apparent interlaminar shear strength	$\tau_{m,13} = \tau_{m,23}$	32,49	<i>MPa</i>
Plain-pin bearing strength	$\sigma_{m,p}$	475,35	<i>MPa</i>
Tensile modulus	E_t	38,51	<i>GPa</i>
Compressive modulus	E_c	39,47	<i>GPa</i>
Flexural modulus	E_f	34,79	<i>GPa</i>
In-plane shear modulus	G_{12}	16,08	<i>GPa</i>
Poisson's ratio in tension	$\nu_{12,t}$	-	-
Poisson's ratio in compression	$\nu_{12,c}$	0,2249	-

5 Discussion

5.1 Comparison to other publications

As discussed in Chapter 2.3, the only sources with which the strengths and engineering constants of the rLFT CF-PEEK material tested here can be compared with are a datasheet for bulk moulding compounds (BMC) from Toray Advanced Composites [15] and a publication by Li and Englund [13]. Figure 5 of the latter shows values for material with pieces between 19,05mm and 12,7mm of about 200 MPa for the flexural and 50 MPa for the tensile strength, while the respective moduli are around 15 GPa and 20 GPa. These values are significantly lower than the results obtained in this master's thesis and this master's thesis cannot give a reason why that is the case.

Table 5.1 gives an opportunity to compare two BMCs from Toray Advanced Composites – the MC1200 and the MS-4H with the rLFT material from this thesis. The latter BMC has an epoxy for matrix, while the former BMC is a carbon fibre and PEEK composite, which, with the exception of the fibre length, should be directly comparable to the rLFT CF-PEEK tested here. With the exception of the compressive strength, the MC1200 BMC has between 10% and 41% higher mechanical properties, which can be explained by the fibre length, which is twice as long as the one in the rLFT material. In the case of the flexural strength, where the difference is higher, two experiments with 2mm plates from the DoE test series yielded strengths of over 600 MPa (N10 and N13). This means it is reasonable to assume, that an rLFT plate made with 25,4mm long fibres and the process used here can achieve similar or higher than the 657,8 MPa one of the MC1200 and the same logic can be applied to the other material parameters. What is interesting to see is that both materials share the same relationships between their flexural, compressive and tensile properties. For both the MC1200 and the rLFT, the compressive modulus is the highest, followed by the tensile and flexural moduli. For the strengths, flexural comes first with compressive in the middle and tensile last. This means, that there are no significant qualitative differences between the compression moulding process for

thermoplastics used by Toray Advanced Composites and the one employed in this master's thesis.

Table 5.1 Material properties of 4mm rLFT CF-PEEK with 12x12mm chips pressed at 395°C and 110 bar, MC1200 PEEK BMC and MS-4H Epoxy BMC [15]

Name	Symbol	rLFT	MC1200	MS-4H	Unit
Density	ρ	1,5763	1,61	1,5	g/cm^3
Fibre content	-	58,78	59	49	<i>vol. -%</i>
Fibre length	-	12	25,4	25,4	<i>mm</i>
Tensile strength	$\sigma_{m,t}$	263,46	288,90	302	<i>MPa</i>
Compressive strength	$\sigma_{m,c}$	348,80	312,30	330,30	<i>MPa</i>
Flexural strength	$\sigma_{m,f}$	467,16	657,80	750,1	<i>MPa</i>
In-plane shear strength	$\tau_{m,12}$	235,30	-	177,90	<i>MPa</i>
Plain pin/bolt bearing strength	$\sigma_{m,p}$	475,35	-	858,4	<i>MPa</i>
Tensile modulus	E_t	38,51	43,40	42,70	<i>GPa</i>
Compressive modulus	E_c	39,47	48,30	50,30	<i>GPa</i>
Flexural modulus	E_f	34,79	40	64,1	<i>GPa</i>
In-plane shear modulus	G_{12}	16,08	-	12,4	<i>GPa</i>

In order to gain a sense of how the in-plane shear and pin bearing characteristics stack up to other similar materials, the rLFT material will be compared to the MS-4H BMC. The in-plane shear strength and modulus of the rLFT material are both around 30% higher than those of the MS-4H BMC. This is despite the fact that almost all other strengths and moduli are higher than those of the rLFT. The testing methodology for the pin bearing strength varies significantly between the two materials, with the rLFT being tested with a free-floating cylindrical pin, while the MS-4H was tested with a bolt, that provides clamping force to the sides of the sample. When compared qualitatively, both materials show a bearing strength higher than the flexural, as well as all other strengths.

Table 5.2 Relative comparison of 12x12mm rLFT pressed at 395°C and 110 bar and the UD tape [16] it is made from

	$\sigma_{m,t}$ [MPa]	$\sigma_{m,c}$ [MPa]	$\sigma_{m,f}$ [MPa]	E_t [GPa]	E_c [GPa]	E_f [GPa]
UD CF-PEEK	2270	1545	1760	141	130	130
rLFT CF-PEEK	263,5	348,8	467,2	38,5	39,5	34,8
rLFT rel. to UD	11,6%	22,6%	26,5%	27,3%	30,4%	26,8%

Table 5.2 gives an overview of the strengths and moduli of the rLFT material relative to the same properties of the UD tape material used in this thesis. The elastic moduli for all three cases are similar and are between 26,8% and 30,4%. The tensile strength is noticeably lower than the compressive and flexural strengths at 11,6% compared to 22,6% and 26,5% respectively. Interestingly, the UD tape has a tensile strength, that is 47% higher than the compressive one, while with the rLFT material the compressive strength is the higher one by 32%.

5.2 Comparison with other lightweight materials

Table 5.3 provides information about the strengths and engineering constants of the high strength aluminium alloy 7075 in T6 heat treated state, the 6061 T6 aluminium alloy, the rLFT CF-PEEK material examined in this master's thesis and the high strength AZ80A wrought magnesium alloy in a T5 heat treated state.

Table 5.3 Material properties of 7075 T6 and 6061 T6 aluminium alloys [15,34], 4mm rLFT CF-PEEK with 12x12mm chips pressed at 395°C and 110 bar and AZ80A T5 magnesium alloy [34]

Name	Symbol	7075 T6	6061 T6	rLFT	AZ80A T5	Unit
Density	ρ	2,81	2,7	1,5763	1,8	g/cm^3
Poisson's ratio	ν	0,33	–	0,225	0,35	-
Tensile strength	$\sigma_{m,t}$	570	310	263,5	380	MPa
Yield stress	$R_{p,0,2\%}$	505	275	–	275	MPa
Tensile modulus	E_t	71	68,9	38,5	45	GPa
Compressive strength	$\sigma_{m,c}$	–	–	349	240	MPa
Compressive modulus	E_c	72,4	69,7	39,5	–	GPa
Flexural strength	$\sigma_{m,f}$	–	–	467	–	MPa
Flexural modulus	E_f	–	–	34,8	–	GPa
Shear strength	τ_m	331	207	235	165	MPa
Shear modulus	G	26,9	–	16,08	17	GPa
Specific tensile strength	$\sigma_{m,t}/\rho$	198,6	114,8	167,2	211,1	Nm/g
Specific compressive strength	$\sigma_{m,c}/\rho$	–	–	221,4	133,3	Nm/g
Specific flexural strength	$\sigma_{m,f}/\rho$	–	–	296,3	–	Nm/g
Specific shear strength	τ_m/ρ	117,8	76,7	149,1	91,7	Nm/g

6061 T6 is a commonly used aluminium alloy which offers good strength and weldability. 7075 T6 is a high strength aluminium alloy, used here to represent the highest strength aluminium alloys out there. Both of these have elastic moduli of around 70 GPa, which is roughly twice that of the rLFT CF-PEEK material with 12mm fibre length. As can be seen from Table 5.1, longer fibres can increase the elastic modulus, but even with 25,4mm long fibres, aluminium is stiffer than long fibre reinforced plastics. The shear modulus of rLFT CF-PEEK is 60% of the shear modulus of 7075 T6, which is still roughly half the stiffness. Where the rLFT CF-PEEK material is comparable or better than the aluminium alloys, is its strength. Excluding the tensile strength, which seems to be the weak point of long fibre reinforced plastics, all other strengths of the rLFT CF-PEEK are better than the ones of the 6061 T6 aluminium alloy. The same can be said for the AZ80A T5 magnesium alloy, which represents here a wrought magnesium alloys with one of the highest strengths among magnesium alloys.

When looking at the specific strengths in Table 5.3, the rLFT material, with the exception of the tensile strength, is superior to the 7075 T6 alloy as well. Specific strength is important for light weight applications, where aluminium and magnesium alloys are very often used exactly because of their high strength to weight ratio. Even the magnesium, with its density not much higher than the rLFT CF-PEEK, has lower specific strength than the rLFT, again with the exception of the tensile strength. The lower tensile strength and elastic modulus of the rLFT can be improved by using longer fibres, which will allow the material to close the gap to the aluminium and magnesium alloys looked at here. One strategy for this would be to tailor the fibre length by only applying longer fibre chips in the key areas, where they are needed. This approach allows a good balance between formability and strength, while also not being too complicated to execute within the compression moulding process. Lastly, the low elastic modulus of the rLFT can be compensated by the geometry of the compression moulded part in applications where stiffness is important. These mechanical properties of the rLFT CF-PEEK material make it a good alternative to aluminium and magnesium alloys, especially when parts from those metals are joined to other carbon fibre reinforced components and galvanic corrosion can occur. Further, the use of a thermoplastic matrix allows parts to be welded together, which is the idea behind the REUSELAGE project – to use compression moulded rLFT parts, that can be integrated into a larger structure during the TP-AFP process.

Another reason why aluminium alloys, such as the 7075 and the 6061, are preferred over other materials is their good corrosion resistance. In this category the rLFT CF-PEEK material excels, because it is not only corrosion free, but also resistant to chemical and solvents [16]. For example, this can be important for applications, where parts are near or in direct contact with salt water.

5.3 Process considerations

As can be seen from Chapter 4.9, due to the large variability of the results from the flexural testing, no conclusion could be drawn if the vacuum positively influences the mechanical strength. Despite the inconclusive result the use of vacuum to prevent oxidation of the PEEK matrix is still advisable, as Day et al. show in [21]. Even though no voids were observed in the samples from the plate processed in air from this master's thesis, compression moulding geometries more complex than a plate could exhibit such problems. LeBlanc et al. did observe voids in the ribbed plate geometry in [19], where the process is done in air. It is reasonable to assume, that such voids will be reduced in size or eliminated if the process took place in vacuum, but this hypothesis could not be proven in this master's thesis.

Another important aspect for an industrial process is the cycle time. The mould and press combination used in this thesis was not able to provide the high heating and cooling rates needed to conduct an experiment in the timeframe that an industrial process will need to have. This in turn means, that the influence of heating and in particular the cooling rate on the mechanical strength could not be examined. The cooling rate in particular is especially important, since PEEK is a semi-crystalline polymer and high cooling rates could cause the PEEK not to crystallize and have an amorphous structure. To avoid that, the manufacturer of the MC1200 CF-PEEK bulk moulding compound, Toray Advanced Composites, recommends in the datasheet [11] a cooling rate of between 5°C/min and 20°C/min in order to maintain the crystallinity of the PEEK polymer.

The square shape of the chips used in this master's thesis is not the norm, when it comes to other publications and BMCs. Both the study done by Selezneva and Lessard [10] and the MC1200 BMC by Toray Advanced Composites have rectangular chips with aspect ratio in the 2 to 8 range. The size and aspect ratio of chips can be controlled freely, when the chips are made by slitting and cutting a UD CF-PEEK tape, but this is not realistic for

a recycling process, since the chips are likely to be created through shredding or hammer milling. Those processes are more likely to produce chips with an aspect ratio of between 1 and 3, meaning square chips or square chips broken in 2 or 3 pieces due to splitting of the UD tape between fibres. Another aspect of chips with medium and high aspect ratios is their tendency to become tangled in one another or form a bundle. Both of these phenomena create a directionality to the fibres in a region of the rLFT plate, which then loses its quasi-isotropic properties, since that assumption is only valid for random fibre orientation.

6 Summary and Outlook

6.1 Summary

This master's thesis deals with the material characterization of a recycled long fibre reinforced thermoplastic consisting of carbon fibre and polyether-ether-ketone. With the increasing use of carbon fibre composite materials comes the need to not only recycle end-of-life parts, but also the production waste generated, which can be up to 20% of the finished part mass. While the recycling of composite materials using thermoset matrix necessitates the separation of fibre and matrix, thermoplastic composites can be directly processed and recycled into new parts. The ability of the thermoplastic matrix to be melted and reshaped is what allows scraps to be compacted into organo-sheets or blocks for further processing. Another option for the recycling of thermoplastic scraps is the compression moulding process, which, through the application of pressure and temperature and the use of a mould with a specific cavity geometry, turns the material into a ready to use part. This thesis examines the mechanical properties of the rLFT CF-PEEK material after it has been compression moulded under vacuum.

Chapter 3 describes the methods and tools used in the course of this master's thesis. It starts with a description of the CF-PEEK material both as received to be used in the recycling process and after the compression moulding. Following that, the compression moulding process is explained in detail, including the equipment used and the experimental procedure. The choice of methodology for the mechanical tests is next, including the tensile, compressive, flexural, bearing strength and shear testing. At the end, an overview of the test series used to determine the optimal set of process parameters for the compression moulding process is given.

Chapter 4 summarizes the results from the DoE test series and the material characterization. It starts with an examination of the rLFT structure, followed by the results of the DoE test series and the parameters chosen for the subsequent testing. The

next section examines the influence of part thickness on the mechanical properties with the use of flexural testing. This is followed by the individual tests carried out as part of the material characterization and lastly a section on the influence of vacuum on strength. Chapter 5 compares the results from the mechanical testing to other publications of compression moulded rLFT CF-PEEK, as well as other materials such as aluminium and magnesium alloys. The rLFT was found to have similar strength to a 6061 T6 aluminium and AZ80A T5 magnesium, as well as comparable specific strength to 7075 T6 aluminium. Lastly, some best practices for how to ensure the compression moulding process yields good CF-PEEK parts are discussed.

6.2 Outlook

The compression moulding process has a great potential as recycling method for CF-PEEK waste, both in a closed loop with TP-AFP and for the manufacture of standalone parts. Some further topics of interest regarding the process include examination of the influence heating and cooling rates have on the crystallinity of the PEEK and the rLFT strength, analysing the difference between processing under vacuum or air further and especially on more complex geometries. Due to the problem with results from a single plate having too much variability, it is recommended to use an average value for the flexural strength from five plates. The use of 4mm or thicker specimen for all further tests is also advised due to the moderate warping most 2mm thick plates manufactured for this master's thesis exhibited. The warping, together with the undulations of the layers could be improved, if better methods for filling the cavity with chips are researched. When it comes to the material parameters, the interlaminar shear modulus G_{13} is of interest for the material modelling, but the testing here was not able to provide a value for it. Additionally, the dependency of the elastic modulus from the process parameters was not captured well by the statistical model and further research into it would be valuable. That study could be combined with a test series similar to the one conducted for the parameter space, where the compaction pressure is replaced by the plate thickness. As Chapter 4.3 showed, thickness does influence the mechanical strength and some combinations of temperature, chip size and plate thickness might yield better results than others.

7 Appendix

Table 7.1 Flexural strengths and moduli of experiments from the DoE test series

Exp. №	T [°C]	p [bar]	CS [mm]	E_f [GPa]	CL 95% [GPa]	CL 95% [%]	$\sigma_{m,f}$ [MPa]	CL 95% [MPa]	CL 95% [%]
N1	380	10	6	32,36	6,78	20,94%	405,48	88,73	21,88%
N2	425	10	6	32,94	4,90	14,87%	438,58	49,76	11,35%
N3	440	10	6	31,80	5,02	15,78%	461,26	34,55	7,49%
N4	380	35	6	30,17	5,85	19,39%	384,88	66,31	17,23%
N5	440	85	6	33,72	3,71	11,00%	420,10	36,54	8,70%
N6	380	110	6	28,97	4,53	15,65%	389,93	28,95	7,42%
N7	395	110	6	30,06	3,42	11,39%	377,90	45,10	11,94%
N8	440	110	6	31,46	2,37	7,53%	413,92	34,38	8,31%
N9	380	10	18	28,30	8,98	31,73%	454,96	107,75	23,68%
N10	440	10	18	39,01	7,61	19,50%	646,79	101,33	15,67%
N11	425	35	18	40,26	11,33	28,13%	593,99	119,27	20,08%
N12	395	85	18	34,41	4,40	12,77%	508,00	67,80	13,35%
N13	380	110	18	38,38	5,23	13,62%	613,10	58,91	9,61%
N14	440	110	18	35,64	7,63	21,40%	554,71	60,00	10,82%
N15	395	10	12	39,29	8,26	21,02%	561,19	112,62	20,07%
N16	440	35	12	32,71	2,45	7,48%	490,44	37,59	7,66%
N17	380	85	12	34,44	5,64	16,39%	469,07	59,04	12,59%
N18	425	110	12	37,82	3,87	10,23%	562,12	50,98	9,07%
N19	410	60	12	32,33	6,92	21,41%	524,80	67,72	12,90%
N20	410	60	12	28,89	5,50	19,04%	471,03	52,01	11,04%
N21	410	60	12	32,26	4,90	15,18%	482,35	40,21	8,34%

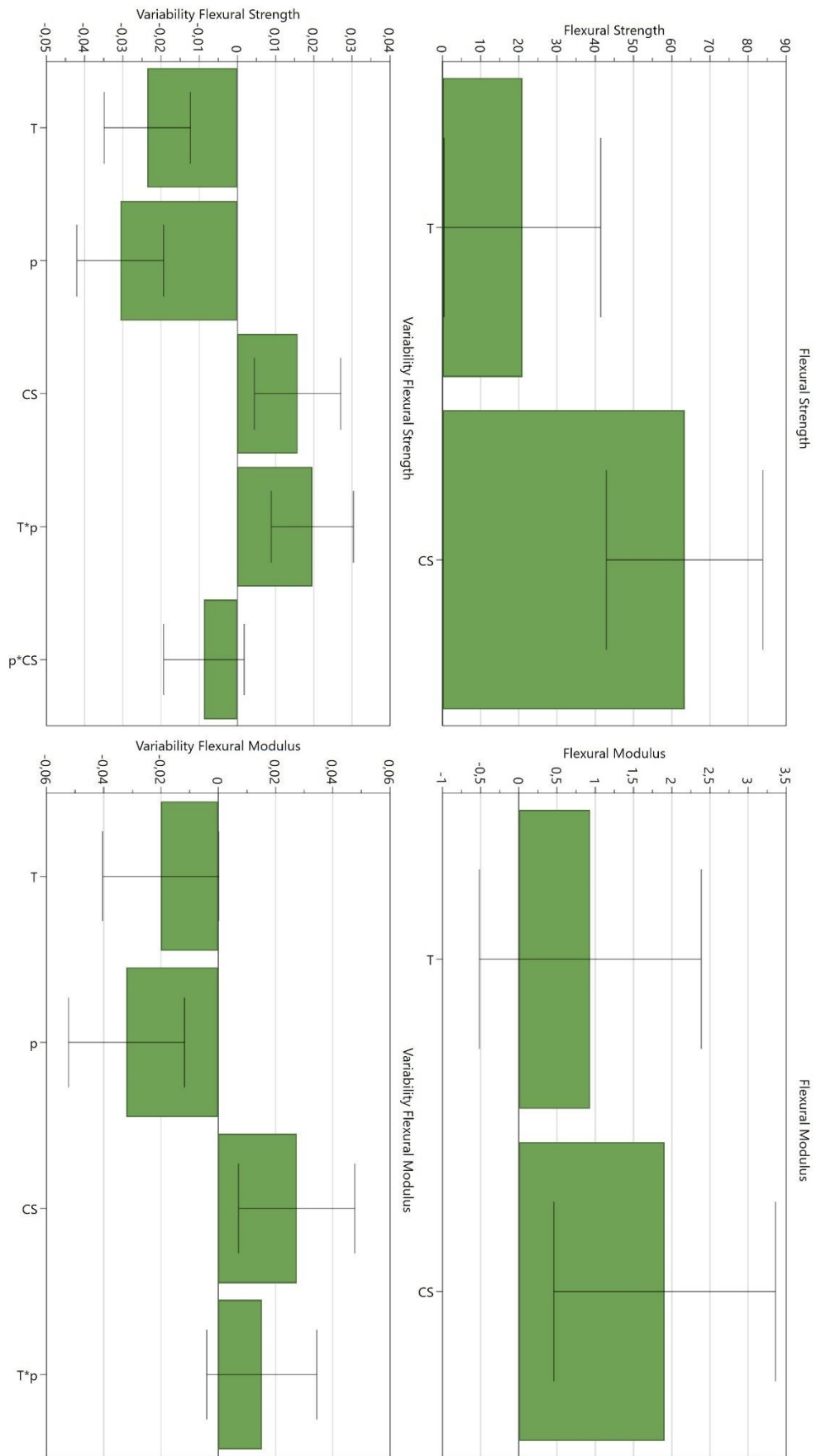


Figure 7-1 Coefficient plot of the statistical model from MODDE

8 References

- [1] Vincent GA. Recycling of thermoplastic composite laminates: The role of processing. Enschede: University of Twente; 2019.
- [2] Lopez-Urionabarrenechea A, Gastelu N, Acha E, Caballero BM, Orue A, Jiménez-Suárez A et al. Reclamation of carbon fibers and added-value gases in a pyrolysis-based composites recycling process. *Journal of Cleaner Production* 2020;273:123173.
- [3] Seiler E, Urban H, Teipel U. Mikrowellenpyrolyse von carbonfaserhaltigen Kunststoffen als Recyclingoption. *Chemie Ingenieur Technik* 2020;92(4):469–75.
- [4] Roux M, Eguémann N, Dransfeld C, Thiébaud F, Perreux D. Thermoplastic carbon fibre-reinforced polymer recycling with electrodynamical fragmentation. *Journal of Thermoplastic Composite Materials* 2017;30(3):381–403.
- [5] Morin C, Loppinet-Serani A, Cansell F, Aymonier C. Near- and supercritical solvolysis of carbon fibre reinforced polymers (CFRPs) for recycling carbon fibers as a valuable resource: State of the art. *The Journal of Supercritical Fluids* 2012;66:232–40.
- [6] Chawla KK. *Composite Materials*. Cham: Springer International Publishing; 2019.
- [7] Schürmann H. *Konstruieren mit Faser-Kunststoff-Verbunden*. 2nd ed. Berlin, Heidelberg: Springer Berlin Heidelberg; 2007.
- [8] Malnati P. Reinforced Thermoplastics: LFRT/GMT Roundup. *CompositesWorld* 2007, 1 August 2007; Available from: <https://www.compositesworld.com/articles/reinforced-thermoplastics-lfirtgmt-roundup>. [June 15, 2022].
- [9] Mallick PK. 2.18 Particulate Filled and Short Fiber Reinforced Polymer Composites. In: Zweben CH, Beaumont P, editors. *Comprehensive composite materials II*, 2nd ed. Amsterdam, New York: Elsevier; 2018, p. 360–400.
- [10] Selezneva M, Lessard L. Characterization of mechanical properties of randomly oriented strand thermoplastic composites. *Journal of Composite Materials* 2016;50(20):2833–51.
- [11] Toray Advanced Composites. Toray Cetex MC1200 PEEK BMC Datasheet.

-
- [12] D. De Wayne Howell, S. Fukumoto. Compression molding of long chopped fiber thermoplastic composites; 2014.
- [13] Li H, Englund K. Recycling of carbon fiber-reinforced thermoplastic composite wastes from the aerospace industry. *Journal of Composite Materials* 2017;51(9):1265–73.
- [14] Tapper RJ, Longana ML, Yu H, Hamerton I, Potter KD. Development of a closed-loop recycling process for discontinuous carbon fibre polypropylene composites. *Composites Part B: Engineering* 2018;146:222–31.
- [15] Toray Advanced Composites. Compression Molding & Bulk Molding Compounds - Advanced Composite Materials Selector Guide.
- [16] Teijin Europe GmbH. Tenax®-E TPUD PEEK-HTS45 Datasheet; 2018.
- [17] Teijin Europe GmbH. Tenax® Filament Yarn Datenblatt.
- [18] Pariyski S. Process Analysis for Compression Moulding with Recycled Thermoplastic CFRP. Term Project. Munich; 2021.
- [19] Leblanc D (ed.). Compression moulding of complex parts using randomly-oriented strands thermoplastic composites; 2014.
- [20] Mothoo J, Ouagne P. Mechanical recycling of continuous fibre reinforced thermoplastic composites using compression moulding: ECCM17 - 17th European Conference on Composite Materials, 26-30th June 2016, Munich, Germany. [Augsburg]: [MAI Carbon Cluster Management GmbH]; 2016.
- [21] Day M, Suprunchuk T, Cooney JD, Wiles DM. Thermal degradation of poly(aryl-ether-ether-ketone) (PEEK): A differential scanning calorimetry study. *J. Appl. Polym. Sci.* 1988;36(5):1097–106.
- [22] Haufler Composites GmbH. HT400+ Datasheet.
- [23] ISO. ISO 527-4 Plastics — Determination of tensile properties — Part 4: Test conditions for isotropic and orthotropic fibre-reinforced plastic composites(527-4:2021); 2021.
- [24] ASTM. D6641 Test Method for Compressive Properties of Polymer Matrix Composite Materials Using a Combined Loading Compression (CLC) Test

- Fixture. West Conshohocken, PA: ASTM International; 2016.
doi:10.1520/D6641_D6641M-16E02.
- [25] ISO. EN ISO 14125 Fibre-reinforced plastic composites. Determination of flexural properties. London: BSI British Standards; 1998.
doi:10.3403/01422801U.
- [26] ISO. DIN EN ISO 20337 Fibre-reinforced plastic composites - Shear test method using a shear frame for the determination of the in-plane shear stress/shear strain response and shear modulus(20337). Berlin: Beuth Verlag GmbH; 2020.
doi:10.31030/3111161.
- [27] ASTM. D7078 Test Method for Shear Properties of Composite Materials by V-Notched Rail Shear Method. West Conshohocken, PA: ASTM International; 2020. doi:10.1520/D7078_D7078M-20E01.
- [28] ISO. DIN EN ISO 14130 Fibre-reinforced plastic composites - Determination of apparent interlaminar shear strength by short-beam method.
doi:10.31030/7433990.
- [29] ISO. ISO 12815 Fibre reinforced plastic composites - Determination of plain-pin bearing strength; 2013.
- [30] Sartorius AB. MODDE 12 User Guide; 2017.
- [31] Melo J, Radford DW. Elastic characterization of PEEK/IM7 using coefficients of thermal expansion. *Composites Part A: Applied Science and Manufacturing* 2002;33(11):1505–10.
- [32] Wang J, Zhou Q, Chao D, Li F, Cui T. In situ determination of mechanical properties for poly(ether ether ketone) film under extreme conditions. *RSC Adv.* 2017;7(14):8670–6.
- [33] Miao Q, Dai Z, Ma G, Niu F, Wu D. Effect of consolidation force on interlaminar shear strength of CF/PEEK laminates manufactured by laser-assisted forming. *Composite Structures* 2021;266:113779.
- [34] ASM International. Handbook Committee. Properties and Selection: Nonferrous Alloys and Special-Purpose Materials. Materials Park, Ohio: ASM International; 1990.